NTIAC-78-2

LIQUID CRYSTALS FOR NONDESTRUCTIVE EVALUATION

by
J. Ivan Ash
Senior Research Engineer
Southwest Research Institute
San Antonio, Texas

September 1978

This document was prepared by the Nondestructive Testing Information Analysis Center (NTIAC), Southwest Research Institute, 6220 Culebra Road, San Antonio, Texas 78284. NTIAC is a full service information analysis center sponsored by the U.S. Department of Defense, serving the information needs of the Department of Defense, other U.S. Government agencies, and the private sector, in the field of nondestructive testing.

NTIAC is operated under Contract DLA900-77-C-3733 with the Defense Logistics Agency. Technical aspects of NTIAC operations are monitored by the U.S. Army Materials and Mechanics Research Center.

UNCLASSIFIED

SECURITY CLASSIFICATION OF THIS PAGE *(When Data Entered)*

REPORT DOCUMENTATION PAGE	READ INSTRUCTIONS BEFORE COMPLETING FORM
1. REPORT NUMBER	2. GOVT ACCESSION NO. AD-A129084	3. RECIPIENT'S CATALOG NUMBER
4. TITLE *(and Subtitle)* Liquid Crystals for Nondestructive Evaluation	5. TYPE OF REPORT & PERIOD COVERED
	6. PERFORMING ORG. REPORT NUMBER NTIAC 78-2
7. AUTHOR(s) J. Ivan Ash	8. CONTRACT OR GRANT NUMBER(s) DLA900-77-C-3733
9. PERFORMING ORGANIZATION NAME AND ADDRESSES NTIAC, Southwest Research Institute P.O. Drawer 28510 San Antonio, TX 78284	10. PROGRAM ELEMENT, PROJECT, TASK AREA & WORK UNIT NUMBERS
11. CONTROLLING OFFICE NAME AND ADDRESS Defense Logistics Agency Headquarters Cameron Station Alexandria, VA 22314	12. REPORT DATE September 1978
	13. NUMBER OF PAGES 40
14. MONITORING AGENCY NAME & ADDRESS *(if different from Controlling Office)* Army Materials and Mechanics Research Center Watertown, MA 02172	15. SECURITY CLASS. *(of this report)* Unclassified
	15a. DECLASSIFICATION/DOWNGRADING SCHEDULE

16. DISTRIBUTION STATEMENT *(of this Report)*

Approved for public release; distribution unlimited.

17. DISTRIBUTION STATEMENT *(of the abstract entered in Block 20, if different from Report)*

18. SUPPLEMENTARY NOTES

For Sale by NTIAC, Southwest Research Institute, P.O. Drawer 28510, San Antonio, TX 78284 ($34.50)

19. KEY WORDS *(Continue on reverse side if necessary and identify by block number)*

liquid crystals, printed circuits, test methods, bond testing, leak detection, acoustic images, integrated circuits, electronic components, thermal properties, components, materials, reviews, history, applications, optical properties, properties, evaluation, NTIAC

20. ABSTRACT *(Continue on reverse side if necessary and identify by block number)*

This document presents a review of the use of liquid crystals in nondestructive evaluation and provides an introduction to the literature. The text begins with an historical background and then discusses the three classes of liquid crystals: the smectic, nematic, a cholesteric or twisted nematic. The properties of liquid crystals are summarized, including optical, thermal, mixtures of different compounds, and dynamic properties. Applications presented include temperature measurement and mapping, thermal mapping, surface

DD FORM 1 JAN 73 1473 EDITION OF 1 NOV 65 IS OBSOLETE

UNCLASSIFIED

SECURITY CLASSIFICATION OF THIS PAGE *(When Data Entered)*

(20) Cont'd.

flaw and leak detection, bond and composite testing, flaw testing with nematics, liquid crystals in fatigue, flow, and fracture tests, fluid flow measurements, acoustic detection and imaging, electronics components and assemblies, RF, microwave, and infrared imaging. The book closes with a bibliography of 84 entries.

NTIAC-78-2

LIQUID CRYSTALS FOR NONDESTRUCTIVE EVALUATION

by
J. Ivan Ash
Senior Research Engineer
Southwest Research Institute
San Antonio, Texas

September 1978

NONDESTRUCTIVE TESTING INFORMATION ANALYSIS CENTER

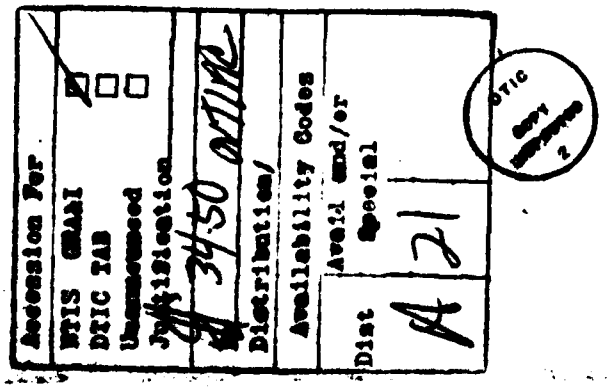

TABLE OF CONTENTS

TABLE OF CONTENTS (CONTINUED)

LIST OF FIGURES

LIST OF FIGURES (CONTINUED)

LIST OF FIGURES (CONTINUED)

LIST OF FIGURES (CONTINUED)

I. INTRODUCTION

A. Purpose

This document presents a review of the use of liquid crystals in nondestructive evaluation (NDE) and provides an introduction to the literature. The technical level of the discussion is such that this document will be useful to the reader who has only an introductory knowledge of liquid crystals in nondestructive evaluation (NDE), but who wants to know what can be done and what is being done in this field. The sophisticated reader can use this document to review, with a minimum expenditure of time and effort, many papers in the field of liquid crystal nondestructive evaluation of materials.

B. Scope

Computer retrieval facilities of the Nondestructive Testing Information Analysis Center (NTIAC) were used to search both the open literature and DDC files. Technical journals, conference proceedings, research reports, Department of Defense technical reports, and trade journals were included in the body of literature surveyed. In selecting documents to be cited in this survey, those which dealt with practical systems and presented experimental data were given primary consideration; thus, no purely analytical papers are included. Almost all of the documents cited in this survey are available in the English language.

C. Organization

This review is divided into three major portions:

1. An introduction to liquid crystals, and their history,
2. A brief summary of liquid crystal properties, and
3. A review of papers discussing liquid crystals in NDE and closely related subjects.

D. Units of Measurement

Throughout the text of this review, Systeme Internationale (SI) units are used in accordance with American National Standard ANSI Z210.1-1976. Approximate English, non SI metric, or in some cases other customary unit equivalents, are frequently included in parentheses following SI units, particularly when the values were originally expressed in the non SI units. In some of the illustrations which are extracted from referenced papers, measurement units used by the authors are retained, and no conversion to SI or English units, as the case may be, is provided. A list of abbreviations for names of units used in this survey is presented in Table I.

II. INTRODUCTION TO LIQUID CRYSTALS

Liquid crystals were discovered in 1888 by an Austrian botanist, Friedrich Reinitzer, when he found that cholesteryl benzoate apparently had two melting points (Ref. 1). At 145°C the solid melted to form a turbid liquid and then, at 179°C, became transparent. In 1889, O. Lehman, a German physicist, identified a molecular structure for this compound which, in the temperature range in question, appeared to be similar to that of a crystal (Ref. 2). Lehman thus coined the term "*liquid crystal*" to denote this phenomenon. Interest in liquid crystals peaked in about 1930 and then decreased.

TABLE I. ABBREVIATIONS FOR UNITS OF MEASUREMENT AND MULTIPLIER PREFIXES USED IN THIS DOCUMENT

NON SI UNITS	SI UNITS	PREFIXES
°F = degree Fahrenheit	°C = degree Celsius	G = giga- = 10^9
in = inch	° = degree (plane angle)	M = mega- = 10^6
ft = foot	Hz = hertz	k = kilo- = 10^3
lb = pound	m = meter	c = centi- = 10^{-2}
G = gauss	min = minute	m = milli- = 10^{-3}
mil = one-thousandth inch	rad = radian	μ = micro- = 10^{-6}
psig = pounds per square inch gauge	s = second	n = nano- = 10^{-9}
CFM = cubic feet per minute	V = volt	p = pico- = 10^{-12}
	W = watt	
	A = ampere	
	T = tesla	
	J = joules	
	Pa = pascal	
	K = kelvin	

However, in the early 1960's there was a resurgence of interest as applications began to emerge and the use of liquid crystals as special materials for studying phase transitions and other phenomena accelerated.

The present classification of liquid crystals was devised by G. Friedel in 1922 (Ref. 3). They are (1) smectic, (2) nematic, and (3) cholesteric, although it is now clear that the latter is a subclass of the second, and may be accurately called "twisted nematic." (Refs. 4, 5). All liquid crystals are actually divided into two types having to do with the manner in which they are produced. "Thermotropic" describes those which are obtained by bringing the temperature of an appropriate compound to the range at which liquid crystalline properties are exhibited and of which the classes smectic, nematic, and cholesteric are subtypes. "Lyotropic" refers to those which are formed by mixing two or more components, one of which, such as water, is polar. Lyotropic liquid crystals have classes designated lamellar, hexagonal, etc. Thermotropic liquid crystals are of primary interest in NDE and subsequent discussion will be limited to them.

Liquid crystal molecules are usually ellipsoidal (cigar-shaped) and bonding forces are generally weak so that crystalline domains can be altered easily and mechanical flow produced. Liquid crystal phases exist only over a limited temperature range, below which the material is a solid and above which it is an isotropic liquid. Within this temperature range the material is anisotropic.

Liquid crystals have some properties normally characteristic of liquids and some normally characteristic of crystalline solids. Molecules in a liquid are randomly oriented to each other while crystals have molecules that have definite orientation and spatial relationships. In general, mechanical properties of liquid crystals appear to be "liquid" (although even their viscosity can be anisotropic, i.e. have directionality, which usually is a sign of crystalline structure), while others, such as optical, electrical, etc., appear to be "solid." Liquid crystallinity is an independent thermodynamic state of matter with reversible phase changes (Refs. 6, 7). It was formerly thought that about 5% of all organic compounds exist in this state, but more recent evidence indicates this number may be closer to 25 or 30% (Ref. 8).

In the smectic (from the Greek word for "soap") class, the long axes of all molecules in a given layer are parallel to each other and perpendicular, or nearly so, to the plane of the layer as shown in Figure 1. Smectic liquid crystals are complex and not so well understood as the other classes, hence having fewer practical applications.

Nematic and cholesteric liquid crystals have been subjected to extensive investigation and their properties are much better known. They both have been used for many practical applications, including NDE. Nematic (from the Greek word for "thread") structures, which are not so ordered as the smectic, are depicted in Figure 2. The long molecular axes are parallel, but there are no layers. Cholesteric (from cholesterol) structures are in layers containing molecules with long axes parallel to the plane of the layer, as in Figure 3, rather than having, as in the smectic form, molecules with long axes perpendicular to the plane of the layer. Molecules of cholesteric liquid crystals are almost flat, but have a side chain of methyl groups which project upward from the plane of each molecule. The displacement required to accommodate this peculiar side chain causes rotation of the direction of the molecules from one layer to the next and results in a helical structure. Cholesteric materials lend themselves more readily to contact thermography NDE by virtue of their unique optical properties, which are

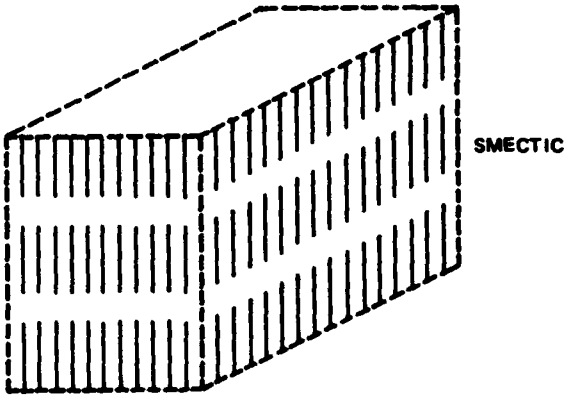

Figure 1. Smectic Liquid Crystal Molecular Form (Reproduced from Nondestructive Testing, A Survey, NASA SP-5113, 1973)

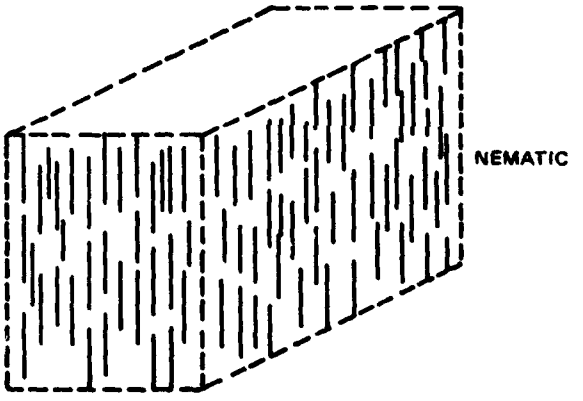

Figure 2. Nematic Liquid Crystal Molecular Form (Reproduced from Nondestructive Testing, A Survey, NASA SP-5113, 1973)

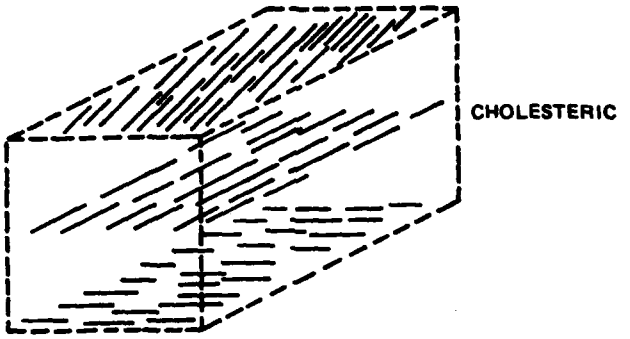

Figure 3. Cholesteric Liquid Crystal Molecular Form (Reproduced from Nondestructive Testing, A Survey, NASA SP-5113, 1973)

discussed subsequently in more detail. They are usually, though not always, formed by derivatives of cholesterol (hence the name "cholesteric"), although cholesterol itself does not exhibit liquid crystallinity.

Both cholesteric and nematic liquid crystals are used in NDE. Areas of application are (1) detection of bulk and surface material discontinuities, (2) detection of semiconductor and electronic component faults, (3) leak detection, (4) detection and mapping of many forms of electromagnetic fields, (5) flow and boundary layer visualization, (6) heat transfer and temperature measurements, and (7) direct visualization of ultrasonic fields being used for inspection, including those from acoustic holography. The use of cholesteric liquid crystals is primarily associated either with temperature induced color changes (for acoustic and electromagnetic field mapping, mechanical motion is converted to heat) or with chemical effects. Nematic crystals generally are used when direct response to mechanical stress (including ultrasonics and static forces) or electromagnetic fields is desired.

III. SUMMARY OF LIQUID CRYSTAL PROPERTIES

Liquid crystals have several distinctive optical properties and undergo interesting changes when subjected to thermal, electric, magnetic, and mechanical fields. Exposure to certain chemicals also produces unique and useful results. Since the molecular structure of liquid crystals is very weak, and thus very sensitive to external forces, even small perturbations can cause dramatic changes. All these properties make liquid crystals useful in a wide variety of applications from optical waveguide and electro-optical devices to NDE. The properties of liquid crystals have been reviewed many times and the reader is referred to the references for a more complete discussion than is given here. In particular, Refs. 4, 6, 9, and 10 should be consulted for a general introduction and Refs. 11, 12, and 13 for analytically oriented reviews.

A. Inherent Optical Properties

The primary optical properties of liquid crystals are (1) optical activity, (2) circular dichroism, and (3) birefringence. These phenomena occur with no external forces or fields applied to the material.

Optical activity, which occurs in cholesteric materials, is the ability of a substance to rotate the plane of polarization of linearly polarized light propagating through it. Total rotation for a given thickness depends on the optical wavelength and the specific liquid crystal material. Cholesteric liquid crystals are the most optically active substances known; it has been reported that the plane of polarization has been rotated as much as 1050 rad (60,000 degrees) in one millimeter (Ref. 6). When compared with the optical activity of quartz, which is considered to have a very pronounced effect, and with other organic liquids, the activity of cholesteric materials can be more fully appreciated. Rotation in quartz at room temperature is about 0.35 rad (20 degrees) per millimeter, while some ordinary organic liquids can rotate the polarization as much as 5.24 rad (300 degrees) per millimeter.

Of all liquid crystals, only the cholesteric structure is circularly dichroic, a property which is usually exhibited only over a limited optical wavelength range. In the circular dichroism exhibited by cholesterics, one circularly polarized component of light is transmitted with no absorption while the other is scattered, although in true dichroism the former component is absorbed (Ref. 14). The component which is affected (left- or right-hand circular polarization) is a function of the specific material. Circular dichroism is the property that determines the characteristic iridescent color of cholesteric liquid crystals when they are illuminated by white light, the color varying with the angle of incidence of the illumination and with temperature. For a given angle of incidence and temperature, the diffracted wavelength approximately follows Bragg's law (Ref. 15). The wavelength of peak intensity for normal incidence and viewing angle is $\lambda = 2np$ where n is the average refractive index in the plane perpendicular to the optical axis and p is the spiral pitch (Ref. 16).

Circular dichroism can be determined by using the equation

$$D = \frac{I_R - I_L}{I_R + I_L}$$

where D is the percent circular dichroism, I_R the intensity of right circularly polarized light and I_L the intensity of left circularly polarized light. I_R and I_L can

be measured directly with a spectrophotometer (Refs. 14, 15). There is also a phase shift between the two components.

All liquid crystal structures are birefringent. Birefringence (or double refraction) is the phenomenon by which light traveling through a material has a velocity dependent upon its polarization. Many polarizers (e.g., Nicol, Rochon, and Wollaston prisms) are based upon this principle. When a beam of unpolarized light impinges on the surface of a birefringent material it is separated into two polarized components (the ordinary, or "o", and extraordinary, or "e" rays) which are at right angles to each other. In liquid crystals, one of these rays has a polarization perpendicular to the long molecular axis of the molecules, and the other has polarization at a right angle to this. These two components travel at different velocities through the material. In effect, each of these components has its own index of refraction according to

$$n = \frac{c}{v}$$

where n is the index of refraction, c the velocity of light in free space, and v the velocity of light in the material. Since v is different for each component, n is different. For some nematic crystals $\Delta n = n_e - n_o = 0.3$, whereas in quartz, $\Delta n = 0.01$. The subscripts e and o refer to the extraordinary and ordinary "rays," respectively. Birefringent crystals are called negative if, as in calcite, $n_e < n_o$, and positive if, as in quartz, $n_e > n_o$. Cholesteric liquid crystals are negative, while nematics and smectics are positive.

B. The Effect of External Influences on Liquid Crystals

1. Cholesterics

Of all the properties of cholesteric liquid crystals, perhaps the best known and most widely used is their change in color as a function of temperature. The wavelength at which scattering occurs, and thus the color seen, can be changed from the ultraviolet to the infrared by changing temperature. However, not all liquid crystals exhibit changes through the full visible spectrum; some have only a limited range and the color sequence may vary with different crystals, even reversing itself. For a given liquid crystal, however, there is a repeatable, one-to-one correspondence between temperature and color.

As discussed in preceding paragraphs, the characteristic color is determined by circular dichroism. At a given temperature the color for a specific liquid crystal or liquid crystal mixture is the same, assuming all other conditions are unchanged. For changing temperature, the twist of the cholesteric structure changes so that the scattered color (wavelength) also changes according to the equation

$$p = \frac{d}{\psi} \times 180^\circ = \frac{\lambda}{2}$$

where p is the distance of alignment or pitch, λ is the peak wavelength of scattered light, d is the spacing of planes, and ψ is the angular shift in degrees between adjacent planes (Ref. 15). Thus, the peak wavelength of the scattered light varies with planar spacing and twist. It seems reasonable that both are affected by temperature changes. In Figure 4, the dependence of the wavelength of maximum scattering on temperature for two pure liquid crystals, cholesteryl decanate and cholesteryl nonanoate, is shown (Ref. 15).

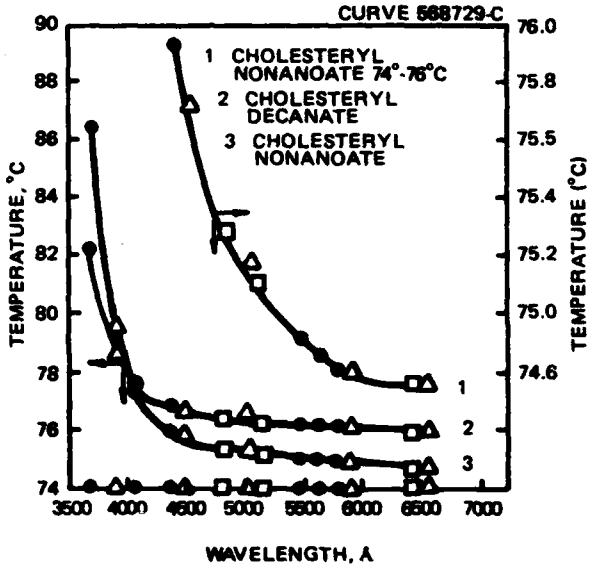

Figure 4. Wavelength of Maximum Scattering as a Function of Temperature for Two Pure Cholesteric Materials (From Ref. 15, Reproduced by Permission of Gordon and Breach, Science Publishers, Inc., N Y)

By mixing cholesterics in varying proportions a desired relationship between color and temperature can be achieved. Figure 5 illustrates the wavelength of maximum scattering as a function of temperature for mixtures of cholesteryl nonanoate and cholesteryl oleyl carbonate (Ref. 17). Curve "a" represents 100% cholesteryl nonanoate and each successive curve a 10% increase in the proportion of cholesteryl oleyl carbonate until curve "k" represents 100% of the latter. It can be seen that for increasing amounts of cholesteryl oleyl carbonate the temperature range over which the color changes occur gets smaller and sensitivity increases. With monochromatic light, temperature changes as small as 0.001 °C have been detected (Ref. 4).

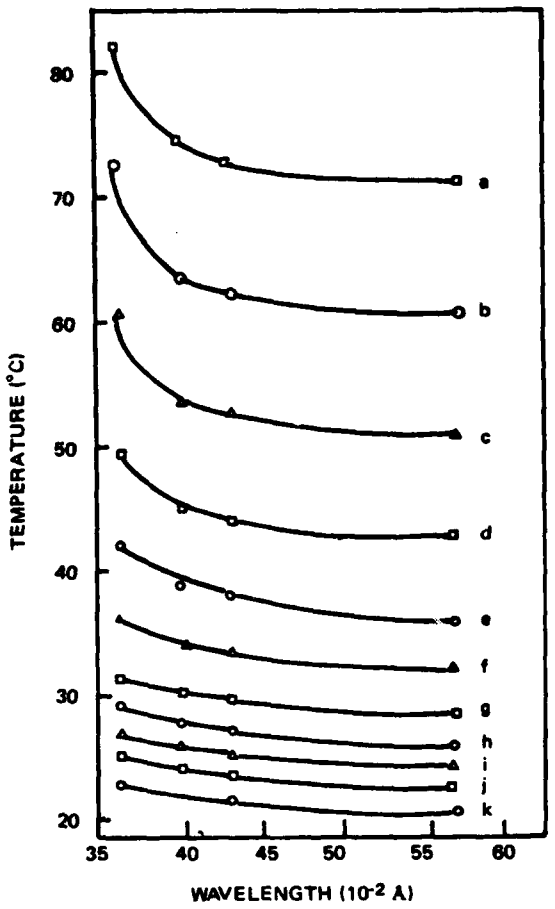

Figure 5. The Wavelength of Maximum Scattering Plotted as a Function of Temperature for Mixtures of Cholesteryl Nonanoate and Cholesteryl Oleyl Carbonate (From Ref. 17, Reproduced by Permission of Optical Society of America, Washington, D C)

There is an additional color changing phenomenon, generally unrelated to the temperature effect, in liquid crystals and liquid crystal mixtures. By adding vapor contaminants, the temperature at which a given color will be seen can be changed, the shift depending on the nature and amount of contaminant. A 4% solution of oleyl amine in a 60/40 cholesteryl nonanoate-cholesteryl oleyl carbonate mixture had a 12°C rise in operating temperature range after a 15 minute exposure to 8 ppm of HCl (Ref. 18). Among numerous chemical vapors which cause this effect are acetone, benzene, chloroform, and petroleum ether (Ref. 10). Two types of changes are possible: (1) the liquid crystals serve as a solvent for a vapor, in which case the color change can be reversed, and (2) the liquid crystal reacts chemically with the vapor or is catalyzed by the vapor, in which case the change is permanent. In either case, the changes appear to be a result of a shift in the birefringence of the cholesteric liquid crystal and can be either to a longer or a shorter wavelength (Ref. 19).

2. Nematics

Both cholesteric and nematic liquid crystals react to induced mechanical stresses. In cholesteric liquid crystals ultrasonic fields can be visualized as color changes by virtue of ultrasonically induced temperature changes, so the mechanism is essentially the same as for temperature mapping. This effect is less pronounced than direct temperature or chemical induced changes (Ref. 9).

In nematic materials the mechanical, ultrasonic, or vibrational stresses are directly responsible for intensity modulation of incident, polarized, monochromatic light (Ref. 16). Mechanical stresses of any sort, including constant pressure, can change the transmitted intensity.

There are numerous electric and magnetic field effects in liquid crystals. Dynamic scattering, field-controlled birefringence, the "guest-host" effect, field-controlled rotation of the plane of rotation, selective reflection, the memory effect, and the electrostructure effect are examples (Ref. 6). Fields which in solid crystals would ordinarily be too weak to align single molecules are strong enough to affect the weak elastic constants of liquid crystals.

There have been many investigations of the effect of fields on nematic liquid crystals. Dynamic scattering, as illustrated in Figure 6, occurs in thin nematic films which are initially transparent. When subjected to d.c. fields of the order of 50kV/m, the light is strongly scattered and appears white. Scattering centers are formed in turbulence caused by the transport of ions through the medium. In "a," the molecules are aligned due to their interaction with the surface of the plates (electrodes). In "b," the media is turbulent and light is scattered. The graph, "c," shows the contrast as a function of voltage for one liquid crystal.

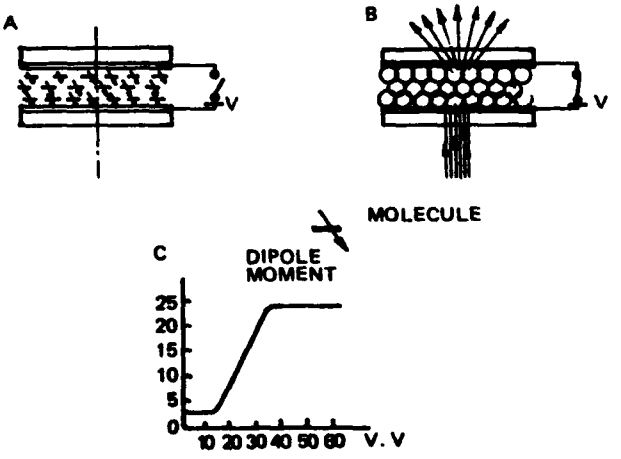

Figure 6. The Dynamic Scattering Effect (From Ref. 6, Reproduced by Permission of Publications Division, American Institute of Physics, N Y)

Field-controlled birefringence in nematics is caused by the reorientation of molecules by the applied field. Since birefringence is caused by certain molecular orientations, a change in such orientation changes the birefringence. The conditions for field-controlled birefringence are:

(1) The liquid crystal layer has homeotropic orientation with no field,
(2) The nematic liquid crystals have negative anisotropy, and
(3) The electric field is parallel to the liquid crystal axis (Ref. 6). Homeotropic orientation means that the optical axes of the molecules are perpendicular to the plates of a cell while homogenic orientation means they are parallel.

Field-controlled rotation of the plane of polarization is, in effect, an electrically induced optical activity (Ref. 6). By proper preparation of a nematic liquid crystal cell, a "twisted" nematic structure can be obtained because the molecules align with the cell walls. For a thick cell the molecules change from one alignment at one wall to another at a second wall. An electric field can undo a twist imposed in this manner, thus undoing the accompanying optical rotation.

If the "twisted" nematic structure associated with field-controlled rotation can be altered by an electric field to give zero degree rotation, then it would seem logical that the "natural" twist of a cholesteric material could also be undone. Theory has been developed to show that large magnetic fields of the order of 10T (100kG) could accomplish this both for cholesterics and for cholesteric-nematic mixtures. Electric fields of the order of 10MV/m have also apparently achieved this untwisting. Less work has been done with electric and magnetic field effects in cholesterics than in nematics (Ref. 12).

The "guest-host" effect refers to the application of electric fields to solutions of some pleochroic dyes (the guest) in nematic liquid crystals (the host) (Ref. 6). Pleochroic dyes are anisotropic in that they have different absorption properties in different directions relative to the molecular axis. When in solution in liquid crystals, the molecules line up with the liquid crystal molecules and change in correspondence with the liquid crystal orientation changes.

The memory effect uses a mixture of nematic and cholesteric liquid crystals and depends on the combination of dynamic scattering of the nematic component and cholesteric hysteresis.

The formation of a mosaic pattern or domain structure in the presence of weak electric or magnetic fields is known as electrostructure (Ref. 6).

IV. LIQUID CRYSTAL NONDESTRUCTIVE EVALUATION

A. Examination of Materials, Components, Assemblies, and Thermal Properties

1. Temperature Measurement and Mapping

Temperature measurements with liquid crystals are useful in scientific and engineering experiments, in medicine and biology, and in nondestructive evaluation. Both point measurements and mapping can be done. Point measurements are frequently associated with medical uses although they are also used in scientific and engineering experiments. Durney, Johnson, and Lords developed a probe, shown in Figure 7, which combines liquid crystals and fiber optics to give a remote temperature measurement capability (Ref. 20). Although designed in this case for making medical and biological measurements where, because of the presence of electric or magnetic fields, thermocouples or other conductive sensors were not acceptable, such combinations of technologies should provide expanded

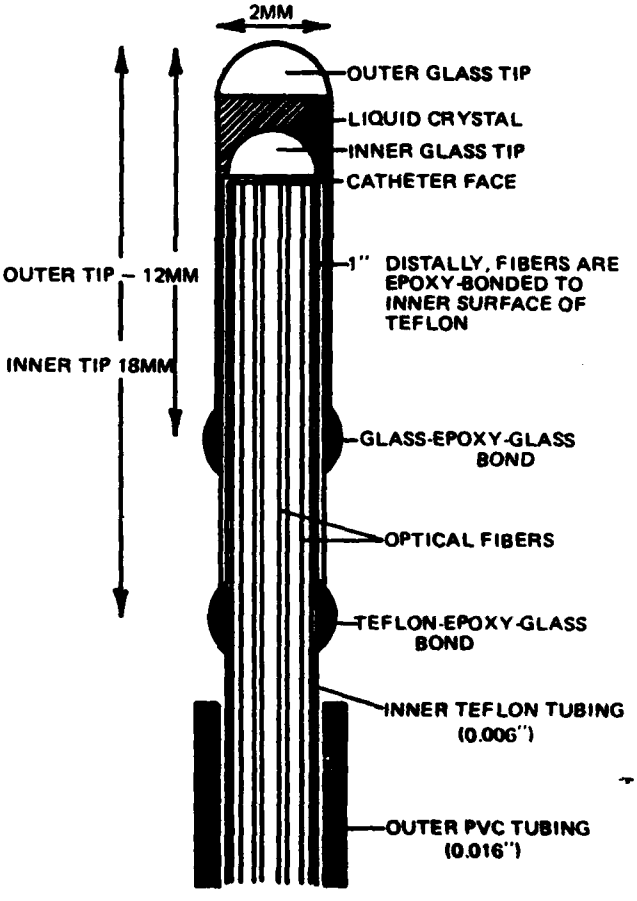

Figure 7. Fiber Optic-Liquid Crystal Sensor Configuration (From Ref. 20, Reproduced by Permission of Office of Naval Research, Washington, D C)

capabilities in nondestructive testing temperature measurements in situations with difficult access. New, low loss fibers now available should make measurements possible even over remote links in excess of 1 km long. Figure 8 illustrates in block diagrams the electronics associated with such a probe. Figure 9 is the calibration curve for three different mixtures of the liquid crystal compounds, cholesteryl chloride, cholesteryl nonanoate, and cholesteryl oleyl carbonate.

Temperature measurement with liquid crystals, including accuracy, resolution, and range, is compared with the use of thermocouples and infrared radiometry in Table II, which is given by Schambeck (Ref. 21).

If cholesteric liquid crystals are to be used to make absolute temperature measurements, they must be calibrated. One method for calibration is illustrated in Figure 10 (Ref. 17). By illuminating the liquid crystal with a monochromatic source and varying the temperature so that the wavelength of maximum scattering sweeps through the source wavelength, the intensity of the scattered light is made to pass through a maximum. The temperature of the block is precisely measured so that the color can be correlated to a given temperature. For the instance reported by Fergason, a mercury lamp with lines at 366 nm, 404.6 nm, 436 nm, 546 nm, and 578 nm was used, an average value being used for the latter two since they overlap. The

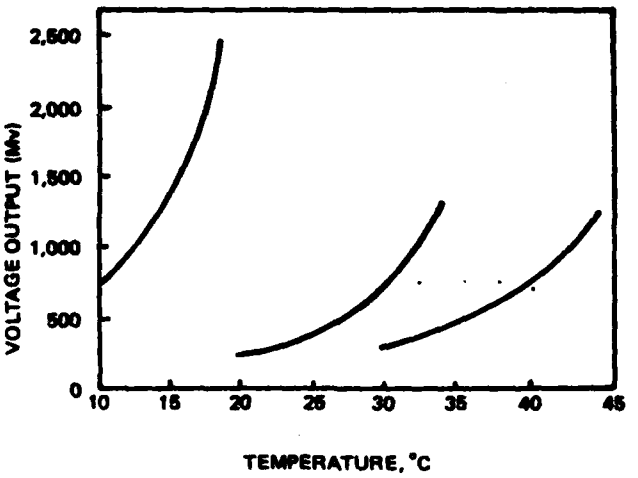

Figure 9. Voltage-Temperature Relationships of Three Liquid Crystal Formulations (From Ref. 20, Reproduced by Permission of Office of Naval Research, Washington, D C)

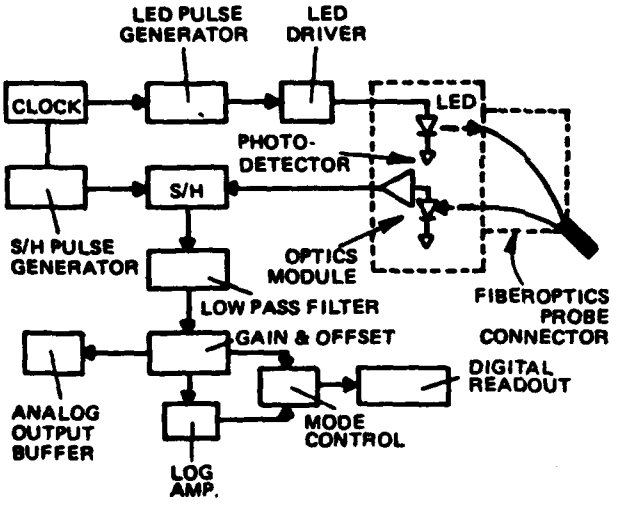

Figure 8. Block Diagram of Fiber Optic-Liquid Crystal Probe (From Ref. 20, Reproduced by Permission of Office of Naval Research, Washington, D C)

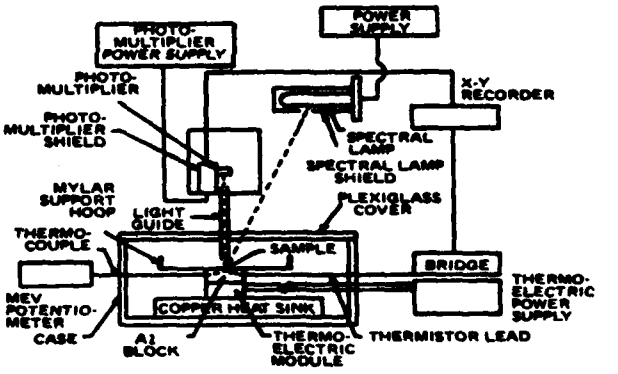

Figure 10. A Block Diagram of an Apparatus Used to Calibrate Cholesteric Liquids for Absolute Temperature Measurement (From Ref. 17, Reproduced by Permission of Optical Society of America, Washington, D C)

TABLE II. CHARACTERISTICS OF SOME TEMPERATURE MEASURING METHODS

	TEMP. ACCURACY	SPATIAL RESOLUTION	TEMP. RANGE	COST
Thermocouples	0.1°C	25.4 μm (1 mil)	<2000°C	$ 1,000
Infrared	0.5°C	12.7 μm (0.5 mil)		10,000
Liquid Crystals	0.1°C	25.4 μm (1 mil)	−20°C to +200°C	1/g

aluminum block was heated and cooled between the temperatures of −10°C to 180°C by a thermoelectric cell, the mode of operation (heating or cooling) being dependent on the direction of current flow. Temperature was measured by a thermistor, the output of which drove the x-axis of an x-y chart recorder. The light intensity was detected by a photodetector and used to drive the y-axis of the recorder. The temperature of each phase transition and the temperature of the scattering peaks was thus obtained. The calibration curves of Figure 5 were obtained this way.

There are other calibration methods which may be used when greater accuracy is necessary. One way is to hold temperature constant and measure reflectance as a function of wavelength using a spectrophotometer. This is a time consuming method requiring expensive equipment (Ref. 17).

As with any test method, the use of cholesteric liquid crystals has certain conditions which must be met if the use is to be effective. A set of six conditions as formulated by Fergason follows: (Bracketed items are inserted to give SI quantities and units).

"(1) The heat capacity of the object should be larger than the capacity of the cholesteric film. The specific heat of most cholesteric materials is 1.5 J/cm^3 [1.5 MJ/m^3]. Since a film of 0.02 mm is required, the heat capacity per centimeter square, which is added to the surface measured, is 3 × 10^{-3} J/cm^2 [30 J/m^2]. In most cases, excepting those involving very thin films, this can be neglected.

(2) The size of the object to be measured must be larger than the limit of resolution of the liquid crystal, thus, a practical limit to the spot size as determined by the liquid crystal is 0.02 mm [20 pm]. In most practical cases, with the exception of integrated circuits, this does not represent a limitation.

(3) The rate of thermal change must be sufficiently slow to allow the cholesteric liquid to follow. Thus, the rate of change of color with temperature has a time constant which is in the neighborhood of 0.1 sec. This represents no limitation for visual observation, however. The time constant must be considered if quantitative information is to be obtained from high speed photography.

(4) The temperature of the object should be in a range where practical cholesteric materials are available experimentally. Liquid crystal materials have been recorded that have color plays from -40° to 285° [°C]. However, this does not represent a practical range for liquid crystals. For most purposes, we might consider the useful range from 0°C to 75°C. Special materials have been made that operate in excess of 100°C and have been successfully applied to semiconducting devices.

(5) If cholesteric liquids are used directly, the surface to which they are applied must be oil resistant. This can best be achieved by use of an oil insoluble film, such as polyvinyl alcohol over the surface.

(6) A final condition on the surface is that it should be black. Since a cholesteric liquid does not absorb light, but scatters it selectively, it is necessary to absorb that light which is not scattered. This condition can be met by either applying a black undercoating or dye." (Ref. 17).

It has more recently become apparent, as will be seen in subsequent discussion, that resolution for testing integrated circuits as cited in (2) is adequate.

By far the largest application of cholesteric liquid crystals has been in thermal mapping for (1) scientific studies of heat flow and distribution and (2) bulk and surface structural flaw testing, the latter a natural extension of the former. Their application to flaw detection of electronic components and materials includes both thermal and electrical properties and is covered in a subsequent section. The great utility of cholesteric liquid crystals for thermal measurements, and particularly mapping, is derived from the dramatic changes in color for very small changes in temperature. Advantages over other methods, in addition to high sensitivity, are (1) low cost, (2) high resolution, (3) simplicity, and (4) speed (Ref. 12). These advantages are outlined briefly:

(1) Low Cost. Liquid crystals themselves are very inexpensive, as can be seen from Table II (Ref. 21). In addition, it is rare that any expensive or elaborate equipment is needed, the eye having sufficient color discrimination for most applications.

(2) High Resolution. The density of thermocouples required to provide equivalent resolution is mind boggling: about one million per square inch would be required. A cost comparison on this basis would also be dramatic.

(3) Simplicity: Beyond developing the ability to apply uniformly thin coatings, the use of liquid crystals is uncomplicated. Airbrushes, found at artist supply stores, are usually used. Tapes with encapsulated liquid crystals or plastic films coated with uniformly thick liquid crystals can be used and the brushing eliminated. The surface should be free of oil soluble material.

(4) Speed. Simplicity usually means speed, and this case is no exception.

Some disadvantages are (1) temperature limitations (maximum useable temperature is 190°C in air and 270°C without air), (2) crystallization and separation of

high temperature materials when at room temperature, and (3) chemical decomposition on exposure to air, even at room temperature (where the limit is 3 to 4 hours exposure). Encapsulation has virtually eliminated deterioration with only small loss of resolution and increase in heat capacity. One system for designating encapsulated liquid crystals uses a letter-number combination such as "R-41." In this case, the "R" (for "regular") designates a nominal visible transition range of 3°C and the "41," the onset of the red transition, 41°C. The letter "S" (for "sensitive") designates a transition range of 1.5°C, and the letter "W" (for "wide"), a range of 6°C. Another solution to the deterioration problem, as reported by Woodmansee, is the use of solid emulsions of liquid crystals dispersed in polymer matrices (Ref. 22).

2. Thermal Mapping

Liquid crystal thermal mapping is useful in studying heat transfer and for NDE. The techniques used in the latter are identical to those for the former, and, in fact, the division is somewhat artificial, since the information obtained from the former is frequently used for the same purpose: (1) design or (2) item evaluation, modification, or repair. In view of this, no rigid differentiation was made, especially where the information was directly transferable to strictly NDE uses.

A rocket motor storage container system was studied by Wirzburger (Ref. 23). The object of the study was development of a model to be used to predict temperature distributions in propellant containers. By using this model, large stresses in the propellant, and thus, possible fractures or poor performance, could be avoided. As part of the study, which included both analytical and experimental techniques, the feasibility of using encapsulated cholesteric liquid crystals in a desert environment to thermally map the surface of the container was investigated.

Prior to applying the liquid crystals, a 38.1 × 50.8 mm (15 × 20 inch) section of the container was sprayed with flat black enamel. It is necessary, in using the scattering of light by cholesteric liquid crystals, to first apply a black or dark coating. (If the liquid crystal should happen to be applied over a reflective surface, the colors which are not scattered could be reflected, thus obscuring or diluting the temperature dependent scattered color.) Then, using a small paint brush, eleven one-inch strips, each of a different temperature range crystal, were applied over the black paint, leaving approximately 12.7 mm (1/2 inch) of black paint between each. A second coat of each liquid crystal was applied after the first was completely dry. After the second coat was dry, two coats of a glossy clear plastic coating were applied to provide some environmental protection. All eleven liquid crystal formulations were calibrated. Two weeks were allowed for the system to stabilize in the outdoor environment.

Both movies and slides were taken with only minor problems caused by reflections from the plastic overcoat. The crystals, after two weeks, maintained their calibration to within ±1.1°C (±2°F). Some adjustments for the increased absorption of the black undercoat were necessary. The use of liquid crystals for thermal mapping under these conditions was considered successful.

The following discussions of heat transfer studies, some of which are essentially extensions of Wirzburger's work, illustrate the types of investigations used to verify the use of liquid crystals for thermal mapping and to determine some techniques and their limits.

A cholesteric liquid crystal thermographic technique was developed by Field to provide both qualitative and quantitative heat transfer information on heated objects in forced convection environments (Ref. 24). The liquid crystals allowed observation and selection of isotherms and inference of the points of flow separation and boundary layer reattachment. A 102 mm (4 inch) diameter right circular cylinder was constructed from 0.99 mm (0.039 inch) thick carbon impregnated paper having a resistivity of approximately 25.4 milliohm meter (1 ohm-in.). The surface of the cylinder was heated by an electric current. The inner hollow space was packed with glass wool to prevent heat losses to the inside. The crossflow of air had Reynolds numbers from 38,000 to 148,000, covering both subcritical and critical flow regimes. The free stream turbulence intensity was approximately 0.5—0.7%. The results were within the experimental uncertainty as predicted by theory and agreed with other experimental work.

McComas (Ref. 25) reported results which supported those of Wirzburger (Ref. 23). Encapsulated cholesteric liquid crystals, previously calibrated by Field, were used for temperature mapping using an experimental method similar to that of Field (Ref. 24).

Cooper, Field, and Meyer have also reported the application of cholesteric liquid crystals to the study of convective heat transfer. Information on the variation of the Nussalt number, and the effects of flow separation, the separation bubble region, the turbulent boundary layer, and the turbulent wake, on surface temperature was obtained for crossflows of air having Reynolds numbers between 40,000 and 150,000. Experimental results agreed with those obtained with more standard techniques. Figure 11 (Ref. 26) demonstrates the method for obtaining data, and the results for the case in which the R-49 liquid crystal was forced to turn red at laminar separation for subcritical flow. The next lower band, the R-45 crystal, had passed through its cycle immediately below the R-49 band, and so on. Only

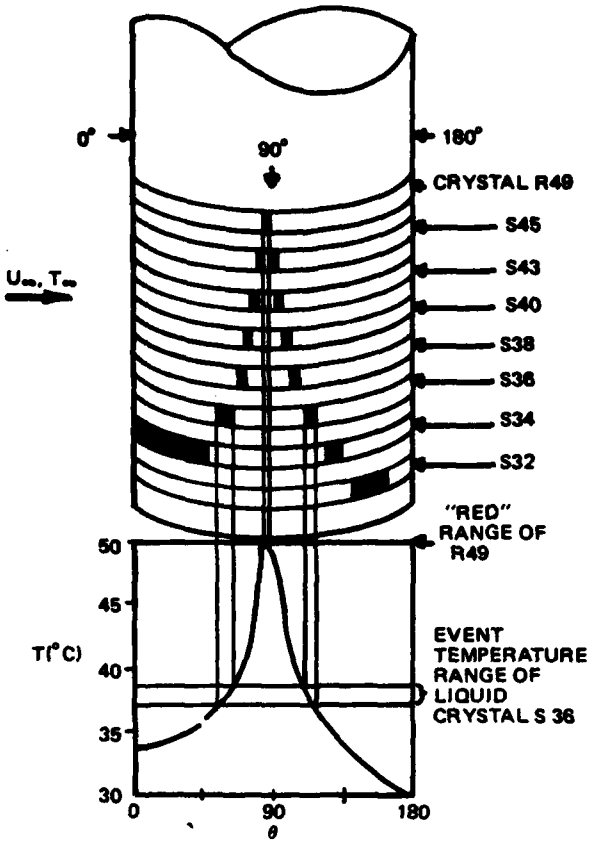

Figure 11. Schematic of Liquid Crystal Measurement of Convective Heat Transfer. The Conditions Depicted are Representative of Subcritical Flow. The Shaded Regions on Each Liquid Crystal Band Represent Color (From Ref. 26, Reproduced by Permission of The American Society of Mechanical Engineers, N Y)

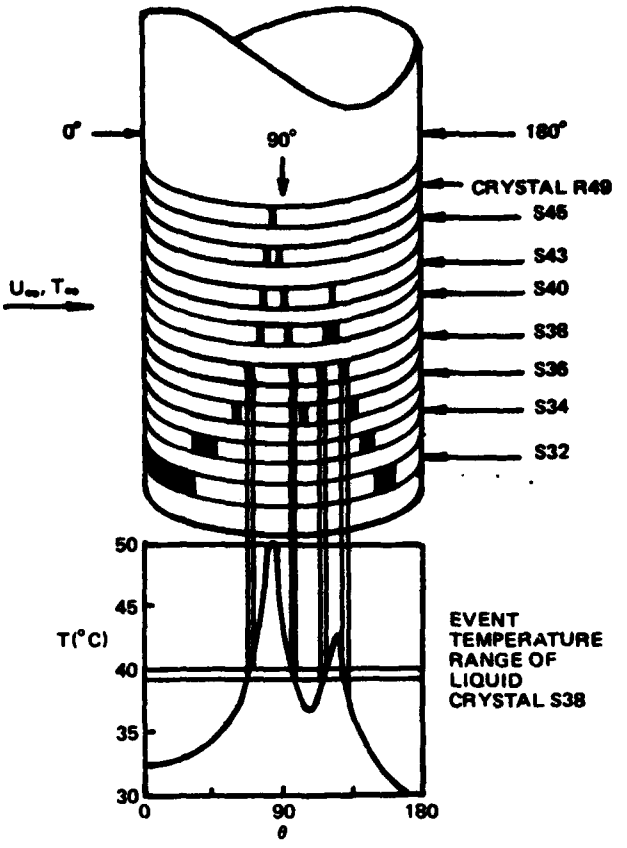

Figure 12. Schematic of Liquid Crystal Measurement of Convective Heat Transfer. The Conditions Depicted are Representative of Critical Flow. The Shaded Regions on Each Liquid Crystal Band Represent Color (From Ref. 26, Reproduced by Permission of The American Society of Mechanical Engineers, N Y)

one colored region was displayed by the S-32 because near the rear stagnation point the cylinder was cooler than near the forward stagnation point. Figure 12 illustrates the same condition for the R-49 liquid crystal, but for critical flow. The appearance of a third colored region for the S-43 liquid crystal and four in subsequent strips, represents the formation of a bubble and the onset of turbulent flow.

Observations of the operation of a gas-loaded variable conductance heat pipe using gases both heavier (krypton) and lighter (helium) than the working fluid (methanol) in both horizontal and vertical positions were made by Batts (Ref. 27). Power input was varied from twenty-five to one hundred fifty watts. The following paragraph excerpted from Batts' report describes the application of the liquid crystals:

> *"The entire condenser section was spray painted with flat black enamel to provide a suitable surface for viewing the transparent liquid crystals. A mixture of equal parts of encapsulated cholesteric liquid crystals R-41, R-49, and R-56 was applied to one side of the pipe using a soft camel's hair brush. Four thin coats were applied, allowing two to three hours drying time between coats. No difficulty was encountered in applying the first two coats uniformly, using the crystals in the aqueous slurry form provided by the manufacturer. For the third and fourth coats, the crystal slurry mixture was diluted with an equal volume of distilled water. This successfully countered the tendency of the material to thicken and roll up during application."*

Isotherms obtained from liquid crystal data are shown in Figure 13 for one set of parameters. The use of liquid crystal temperature mapping was considered successful by the experimenter.

The effect of gravity on gas-loaded variable conductance heat pipes has been further studied by Kelleher on three heat pipes using methanol or Freon 113 as the working fluid and krypton or helium as the control gas

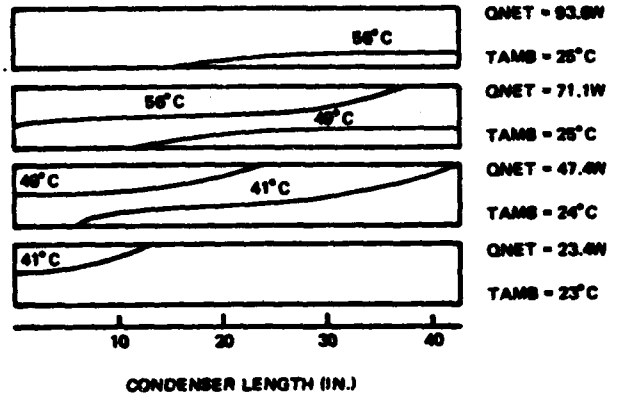

Figure 13. Liquid Crystal Isotherms–Horizontal–.00607 lbm Krypton (From Ref. 27, Reproduced by Permission of Research Library at Naval Postgraduate School, CA)

(Ref. 28). The usual technique for this experiment consists of using a string of thermocouples in a single axial line, assuming that the temperature, and thus the distribution of fluid concentrations, is nearly one-dimensional and varies only with the axial coordinate. These tests showed that gravity distorted axial temperature profiles even on a small diameter (16 mm) heat pipe and caused a stratification of work fluids and control gases in a larger (50-mm diameter) one. Figures 14 and 15 show the liquid crystal isotherms for a 50-mm diameter pipe in the vertical and horizontal positions, respectively, using a methanol working fluid and a helium control gas.

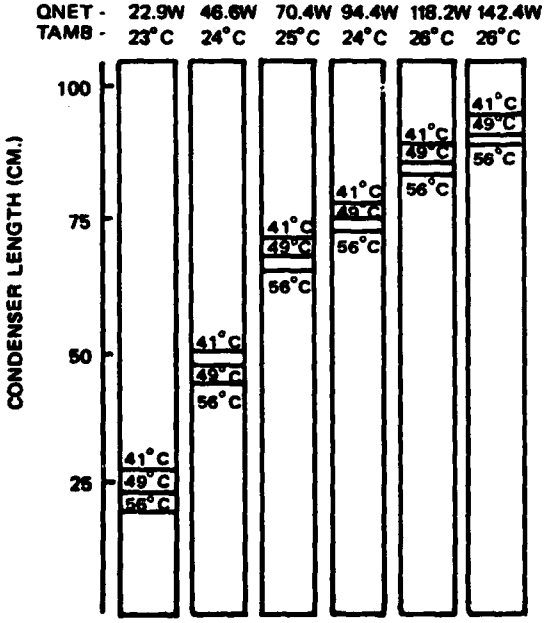

Figure 14. Liquid Crystal Isotherms for a Vertical 50 mm Diameter Pipe Using Methanol with 0.182 gm Helium (From Ref. 28, Reproduced by Permission of Research Library at Naval Postgraduate School, CA)

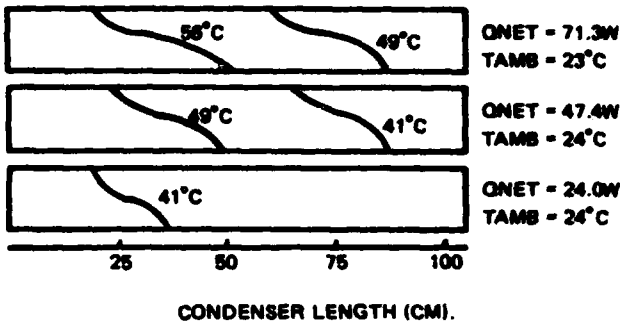

Figure 15. Liquid Crystal Isotherms for a Horizontal 50 mm Diameter Pipe Using Methanol with 0.182 gm Helium (From Ref. 28, Reproduced by Permission of Research Library at Naval Postgraduate School, CA)

Owendoff used heat pipes in both conventional and variable conductance operation to gather experimental data and determine performance characteristics (Ref. 29). In the variable conductance mode, liquid crystals displayed qualitatively the temperature gradients occurring across the vapor-gas interface and gave results similar to those reported by Kelleher (Ref. 28).

The techniques demonstrated in these preceding studies are important to NDE because they demonstrate the ease with which mapping can be accomplished and show that significant quantitative data can be obtained using liquid crystals.

Woodmansee demonstrated the use of cholesterics to test isolation of the tapered portion of aluminum rivets as illustrated in Figure 16 (Ref. 30). A liquid crystal having a range of 30 °C was applied to the rivet head. If the rivet's zinc chromate coating was sufficient, the liquid crystal turned violet in about 2 seconds. Inadequately coated rivets took as much as 20 seconds or longer.

Woodmansee also reports that heat exchanger obstructions or constrictions which are close to an accessible surface have been detected by observing the

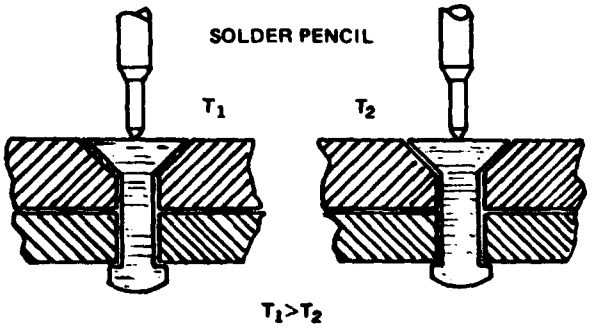

Figure 16. Thermal Testing of Fastener Insulation with Liquid Crystals (From Ref. 30, Reproduced by Permission of The American Society for Nondestructive Testing, Inc., Columbus, OH)

surface temperature pattern while simultaneously cycling the coolant temperature (Ref. 22). Deposits of organic substances were creating obstructions in a panel as shown in Figure 17 (Ref. 22). The panel was made of

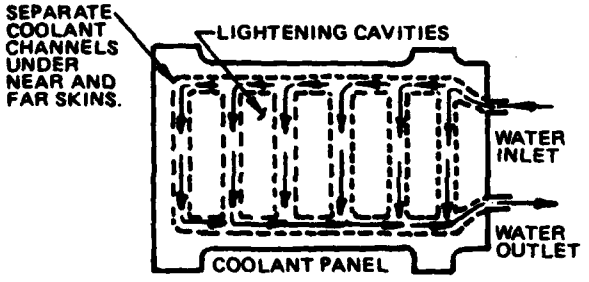

Figure 17. Liquid Crystal Thermal Test of Coolant Panel (From Ref. 22, Reproduced by Permission of Optical Society of America, Washington, D C)

aluminum sheets 0.5 mm thick between which were diffusion bonded 6-mm wide ribs with intervening cavities for weight reduction. Slots for coolant flow 0.6 mm wide and 2 mm deep were machined along the rib centerlines on both sides. A header system at both top and bottom of the ribs supplied coolant. Pins placed in the slots were used to simulate obstructions. Hot and cold tap water were alternately caused to flow through the channels. Cholesteric liquid crystals were coated on one surface of the panel. On the uncoated side of the panel a single channel obstruction was simulated. Complete obstruction was easily detected, but detection of partial obstruction was more difficult.

3. Surface Flaw and Leak Detection Using Chemical Contamination and Thermal Properties of Cholesterics

Cholesteric liquid crystals have been used by Woodmansee and Southworth for flaw detection both as an adjunct to liquid penetrants and as an independent vehicle (Ref. 31). Figure 18 illustrates the effect of kerosene and the penetrant ZL30A on the red transition temperature of one sample. For many reasons, normal penetrant use can be less effective than required, but the reaction of liquid crystals to penetrants can increase this effectiveness. Liquid crystals were applied to detect the presence of penetrant residues within cracks which were otherwise not visible over the full extent of a crack. In one case a titanium alloy marine propeller failed in service and repeated examination by penetrants gave decreasingly satisfactory results until aided by liquid crystals. In another case, liquid crystals were used to provide clear indications where a liquid penetrant was applied to a severely cracked submerged arc weld in a maraging steel plate after use of magnetic particles.

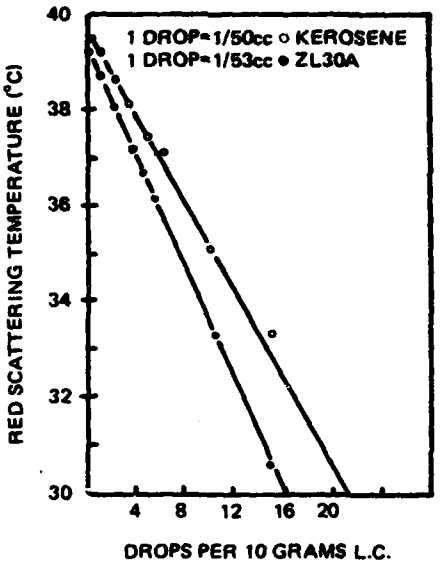

Figure 18. Effects of Contaminants on Transition Temperature of Cholesteric Liquid Crystals (From Ref. 31, Reproduced by Permission of The American Society for Nondestructive Testing, Inc., Columbus, OH)

Unsatisfactory indications were obtained with the penetrant until kerosene and liquid crystals were used. In a later test the kerosene was omitted and the liquid crystals still enhanced the indication to a satisfactory level.

Another test was conducted by Woodmansee and Southworth to test the vacuum tightness of resistance roll-seam welds (Ref. 31). Type 321 annealed corrosion-resistant steel 1.525 mm (0.060 in.) thick was used for the container. The contaminating gas, acetone, was injected to a gauge pressure of 3.4 kPa (5 psig). Gas escaping through small leaks was qualitatively detected using cholesterics.

Liquid crystals have been used to detect chemical vapors in concentrations on the order of a few parts per million. This capability is useful for qualitative and quantitative analysis of enclosed atmospheres, detection of contaminants, and spectroscopy, as well as leak detection. Foreign vapors affect phase transitions, dichroic properties, and polarization, and can cause fluorescence. Both cholesteric and nematic liquid crystals have been investigated for this application.

Surface or subsurface cracks or discontinuities may alter heat flow enough to distort temperature distributions. Figure 19 illustrates such a test using liquid crystals (Ref. 30). A beryllium clip containing a crack was heated with detectable results as shown. There was a heat build-up on the heated side of the crack.

Woodmansee and Southworth also described the use of the thermal cholesteric properties of the liquid crystals for detection of discontinuities in thin, 1.015

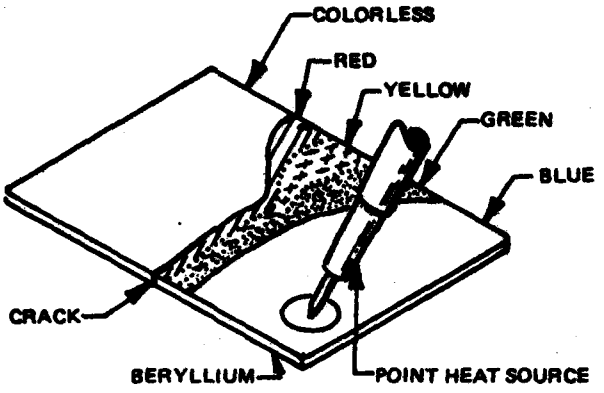

Figure 19. Crack Detection with Liquid Crystals (From Ref. 30, Reproduced by Permission of The American Society for Nondestructive Testing, Inc., Columbus, OH)

mm (0.040 in.) sheets of titanium, copper, and aluminum (Ref. 31). A 25 mm (1 in.) long slot was machined in the center of the plate and the surface painted with liquid crystals. The effect of these artificial cracks on heat flow is shown schematically in Figures 20 and 21 (Ref. 31) for stationary and moving point heat sources, respectively. The isotherm spacing may vary for materials with different thermal conductivities. Thermal detection is superior to penetrant detection when the crack is smeared or subsurface, and in fatigue cycling tests. In the latter, the generation of heat associated with the formation and growth of cracks supplies the heat for color changes, an application which is discussed more fully in following pages.

Manaranche, in 1973, reported a comparative study of four methods for NDE of welds: (1) mechanical impedance, (2) liquid crystal, (3) eddy currents, and (4) potential measurement (Ref. 32). Figure 22 illustrates the method used to investigate liquid crystals. A heat flux, which shifts in accordance with the direction of the axis of revolution, was sent through the weld bead.

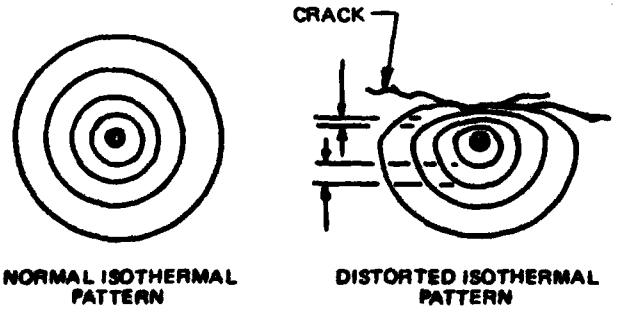

Figure 20. Isothermal Pattern for a Stationary Point Heat Source (From Ref. 31, Reproduced by Permission of The American Society for Nondestructive Testing, Inc., Columbus, OH)

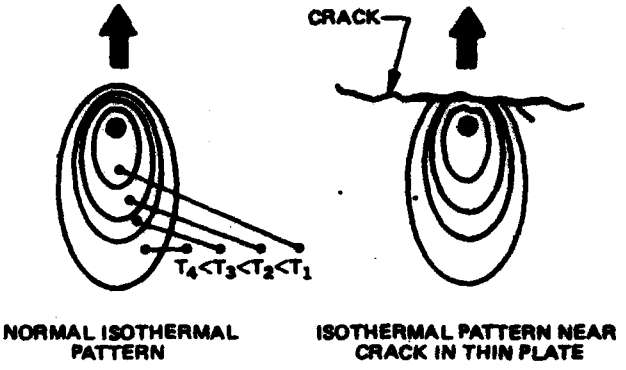

Figure 21. Isothermal Pattern Around Moving Point Heat Source (From Ref. 31, Reproduced by Permission of The American Society for Nondestructive Testing, Inc., Columbus, OH)

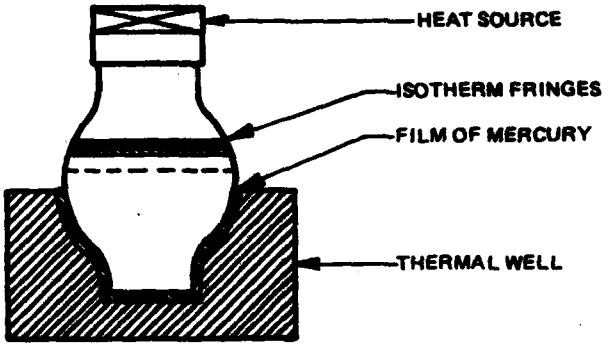

Figure 22. Set-Up for Evaluation of Liquid Crystal Weld Testing (From Ref. 32, Reproduced by Permission of British Institute of Nondestructive Testing, Southend-on-Sea Essex, England)

While the temperature was rising, the evolution of isotherms in the weld bead vicinity could be observed. The heat source was a wirewound resistor and the heat sink, a metallic mass. Where there was no longitudinal crack, the evolution of the isotherm, and thus, color fringes developed along parallel circles. Any fissure distorts and thins out fringes. Manaranche's conclusion was that the four methods investigated were complementary.

4. Bond and Composite Testing

Metal-to-metal adhesive bonds in aluminum stiffener panels were inspected by Woodmansee (Ref. 30). A mixture of cholesteric liquid crystals, with properties similar to those of mixture A of Figure 23, was applied to a panel over a thin coat of black paint. The poorer heat conduction of bond voids caused the surface temperature over these areas to rise more slowly than in well bonded areas. Heat was applied to one side of the panels and the temperature distribution was observed on the opposite. Figure 24 illustrates the color changes observed in a uniformly bonded 50 × 280 mm (2 × 11 in.) strip of panel during the application of heat and the

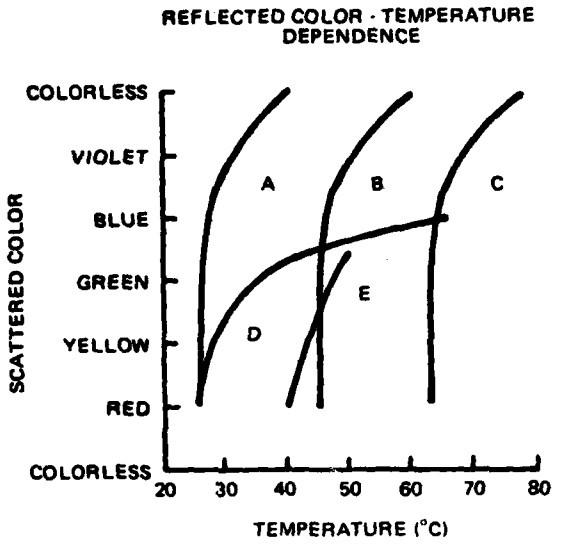

Figure 23. Temperature Dependence of Light Scattering for Mixtures of Cholesterol Esters (From Ref. 30, Reproduced by Permission of The American Society for Nondestructive Testing, Inc., Columbus, OH)

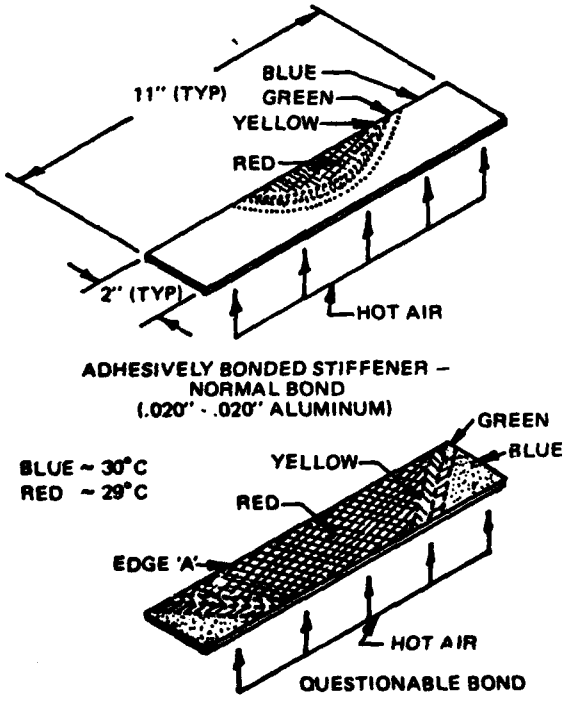

Figure 24. Color Pattern for Uniformly Adhesively Bonded Aluminum Stiffeners (From Ref. 30, Reproduced by Permission of The American Society for Nondestructive Testing, Inc., Columbus, OH)

distribution at the end of a seven-second heating period. Figure 25 shows the distribution and void area for a flawed panel.

Honeycomb sandwich materials have been inspected by Woodmansee with cholesteric liquid crystals (Ref. 30). Figure 26 illustrates an aluminum honeycomb panel in which Teflon patches were inserted to simulate flaws.

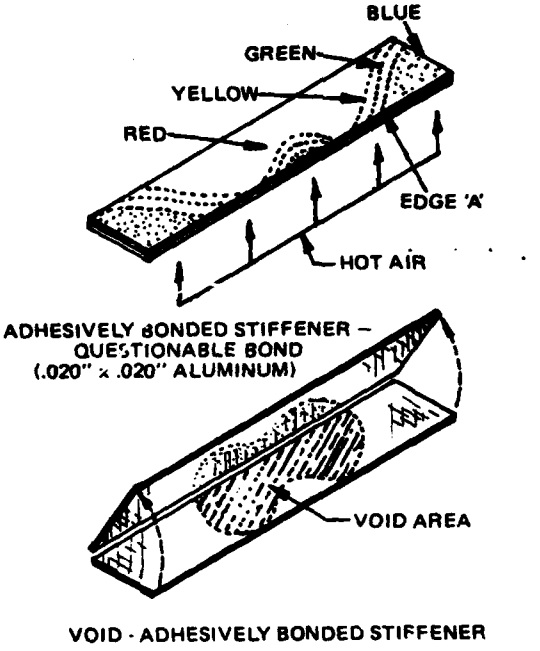

Figure 25. Void Detection in Adhesively Bonded Aluminum Stiffeners (From Ref. 30, Reproduced by Permission of The American Society for Nondestructive Testing, Inc., Columbus, OH)

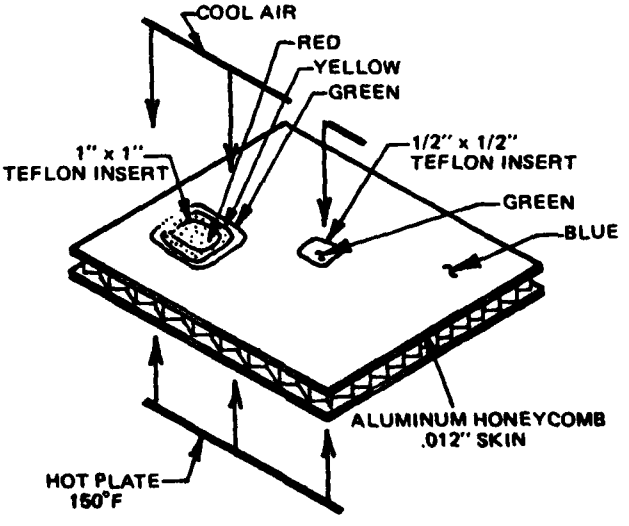

Figure 26. Visualization of Teflon Inserts in Aluminum Honeycomb (From Ref. 30, Reproduced by Permission of The American Society for Nondestructive Testing, Inc., Columbus, OH)

The lower face was on a hot plate maintained at 66 °C (150 °F) and the upper surface was convectively cooled to remain in the liquid crystal temperature range. Patches as small as 12 × 12 mm (1/2 × 1/2 in.) were observable, but 6 × 6 mm (1/4 × 1/4 in.) patches were not.

A report by Cohen described procedures and equipment for conducting thermographic tests using liquid crystals as indicators (Ref. 33). A total of 27 m^2 (290 ft^2) of bonded honeycomb and laminated metallic and nonmetallic structural panels with built-in flaws were tested to determine concept feasibility. The technique was proven to be feasible in applications that would otherwise require more complex and costly systems. The equipment and techniques do not require highly trained personnel.

The detection of a series of small voids for a titanium face sheet 0.5 mm thick and an aluminum honeycomb core was investigated by Woodmansee (Ref. 22). When the face sheet was radiantly heated, the area over the voids was at a higher temperature and when cooled with an air hose, cooled more rapidly than properly bonded material. Further bonding anomalies could be detected by disturbances of the regular pattern. To facilitate the application of liquid crystals to extensive areas, the investigator developed a mixture of liquid crystals and approximately 20-30% by weight filler material such as Tempera, black paint, or carbon black. This mixture was applied to a surface in a single coat. All color transitions were observable with the mixture, though they were less intense than with clear liquid crystals applied over flat black paint.

Also, vacuum techniques were developed to hold liquid crystal films against surfaces (Ref. 22). A polyvinyl alcohol film, 25 μm thick, was bonded to a continuous loop of vacuum tubing with epoxy. A series of holes were drilled in the inside wall of the tubing, which serves as a vacuum manifold and the tubing was connected to a vacuum line via a section of copper tubing. The assembly could be moved over the surface being inspected. Other forms of this arrangement had been used.

Forman has reported successful testing of composites (Ref. 34). The minimum detectable defect for those having 1.525 mm (0.060 in.) skins was one crushed cell of 1.6 mm (1/16 in.) and for 4.825 mm (0.190 in.) skins it was 650 mm^2 (1 sq. in.). The following were tested:

(1) Aluminum skins with high temperature phenolic honeycomb core,
(2) Glass cloth skins with glass fiber honeycomb core,
(3) Titanium skins with aluminum honeycomb core,
(4) Titanium skins with high temperature phenolic honeycomb core, and
(5) Glass cloth laminates.

He reported that incandescent lighting is better than fluorescent, (because of the continuous output spectrum), although in most cases the latter is adequate. Also, he stated that simultaneous heating and cooling as, for example, when a test panel is heated on one side and cooled on the other, give better results. He used a water soluble black base coat to provide an optimum reflectance surface. Benzene, toluene, chloroform, or petroleum ether were used as solvents for the cholesteric crystals. A brush or a spray gun was used for application with spraying recommended for large panels. Cholesteric crystals were reclaimed by redissolving from the test surface with common organic solvents and the black coat was removed with water.

The use of ROCHROME liquid crystal tape for thermographic testing of bonded structures for aircraft was demonstrated, including techniques for applying the tape, heating test panels and photographing resulting thermal patterns (Ref. 35). Results were similar in quality to those obtained by direct application to the surfaces, though resolution was not as good.

Nondestructive inspection using blended cholesteric esters was reported by S. Brown (Ref. 36). The sensitivity range (1 °C) of available liquid crystals was adequate for thicknesses of 0.510 mm (0.020 in.) or less, but not small enough for composite structures with aluminum skins as thick as 1.525 mm (0.060 in.). Blends having full color ranges of 0.5 °C and as small as 0.1 °C were evaluated on aluminum honeycomb composite structures with simulated debonds. Three types of defects, (1) oil on the inner surface of the skin (simulated by a teflon insert), (2) crushed core, and (3) cured adhesive, were investigated, with the first being the hardest to detect. Some blends worked well on the entire range of skin thicknesses from 0.510 to 4.825 mm (0.020 to 0.190 in.). The minimum definable defect for a 1.525 mm (0.060 in.) skin was one crushed honeycomb cell of 1.6 mm (1/16 in.) whereas for 4.825 mm (0.190 in.) skins it was 650 mm (1 sq. in.). These results are similar to those of Forman (Ref. 34). Voids near the surface were easier to detect. Other composites successfully investigated were:

(1) Aluminum skins with HRP (high temperature phenolic) honeycomb core
(2) Glass cloth skins with fiber honeycomb core
(3) Titanium skins with aluminum honeycomb core
(4) Titanium skins with HRP core
(5) Glass cloth laminates

Additional findings were that incandescent lighting works better than fluorescent, and simultaneous heating of one surface and cooling of the other enhanced the effect.

Other applications cited were:

(1) detection of electronic hot spots
(2) checking special insulation required to prevent contact of dissimilar materials
(3) determination of human skin temperature variations

Conclusions of this study were that (1) the technique was useable for many composite structures in production, and that (2) cholesteric liquid crystals potentially provide simple, reliable, and economic evaluation of bond defects in composite structures.

Bekeshko reported the use of liquid crystals to identify weak bond sites in metal-to-metal adhesive joints (Ref. 37). Poor adhesive bonding areas of 6 mm diameter were found in joints between 0.5 mm thick aluminum plates and 2 mm thick copper plates heated to 68 °C with a temperature difference of 7 °C.

More recently, Schaum has reported the development of encapsulated cholesteric liquid crystal inspection techniques for advanced composite materials (Ref. 38). Preliminary investigations of the thermal conductivity of a 1.04 mm (0.041 in.) thick graphite/epoxy laminated panel in directions both normal and parallel to the composite laminate were made with thermocouples being used for measurements of the former and liquid crystals for the latter. Panels with intentionally introduced flaws were tested. A graphite/epoxy panel having 8 plies shown in Figure 27 was constructed from NARMCO Rigidite 5208-UCC Thornel 300 prepreg tape. Sixteen Teflon triangles were introduced as artificial flaws. The shape and size of the triangles were selected to allow investigation of different tapers.

By comparing the shape of the surface temperature pattern with the known shape of the Teflon triangles, it was hoped that quantitative evaluation of the liquid crystal technique could be obtained. As can be seen from Figure 28, the Teflon triangles were made of four different thicknesses of t, 2t, 3t, and 4t, where t was the thickness of the thinnest and a flaw thickness range from 6% to 21% of the finished panel thickness was used. Four Teflon triangles of different thickness and identical shape and area were placed in each of four interlaminar interfaces. Observation from both sides gave data for every possible flaw depth.

The triangles were laid on a carefully measured grid which was marked by implanting 50.8 μm (0.002 in.) wires in the 12.7 mm (0.5 in.) border of the panel. The panel surfaces were sprayed with flat black enamel and, when dry, with encapsulated cholesteric liquid S-30. The panel was mounted vertically in a small vise and the opening of a large tubular polyurethane plastic bag was attached to the edges of the panel with long strips of U-shaped plastic molding which left 38.1 mm (1.5 in.) openings at the corners of the panel. A 38.1 mm (1.5 in.)

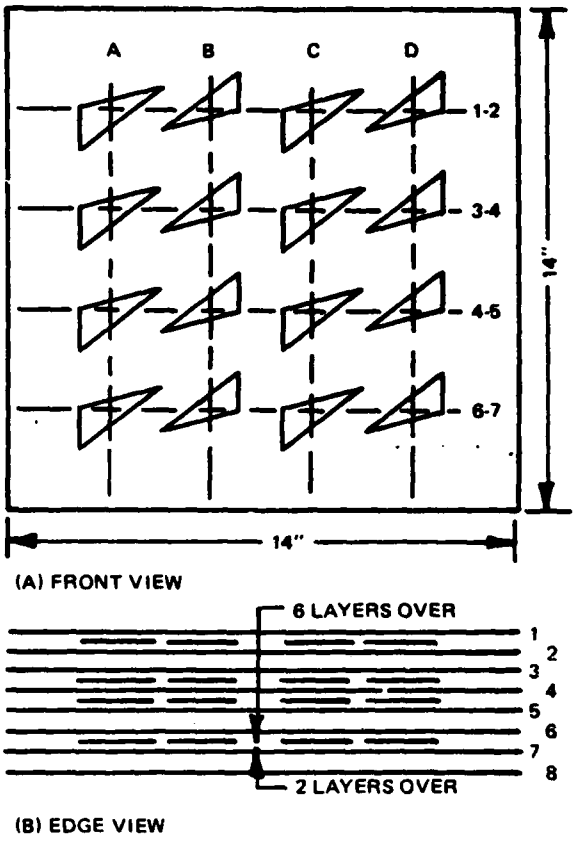

Figure 27. Graphite/Epoxy Laminate Test Panel (From Ref. 38, Reproduced by Permission of the Research Library of the Naval Postgraduate School, CA)

diameter hose was attached to the other end of the bag. A smaller perforated plastic bag was attached to the end of the hose so that warm air passing into the larger bag would be effectively diffused. A small, low velocity heater-blower unit capable of heating air to 70 °C was attached to the other end of the hose. The large bag was slightly pressurized with warm air which soon reached a near steady state condition when the blower was on, thus providing nearly uniform heat over the rear surface of the panel.

Although holding surface temperatures within 2 °C tolerance at 30 °C was not possible, fifteen of the triangles were observed in their undistorted shapes under the very slow changes achieved. Since actual flaw detection capability was the primary goal, a 2 °C tolerance was not necessary. Enhancement of the thermal pattern was accomplished by pulsed heating (or cooling) of the local surface above flaws. Sensitivity sufficient for detection of surface temperature differences between areas above the flawed and unflawed regions within approximately 0.5 °C was achieved.

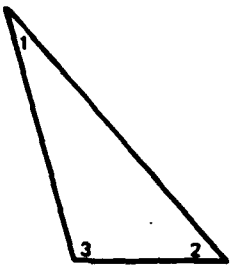

∠1 = 26°
∠2 = 51°
∠3 = 103°

AREA = 1.0 IN²

TYPE	THICKNESS, IN.	% D *
A	.009	21.4
B	.0065	15.4
C	.0045	10.7
D	.0025	6.0

*D = FINISHED THICKNESS OF PANEL

Figure 28. Teflon Triangles (From Ref. 38, Reproduced by Permission of Research Library at Naval Postgraduate School, CA)

5. Other Materials and Items

Other NDE temperature mapping applications of cholesteric liquid crystals have been explored. Best has reported the testing of helicopter tail rotor blades using cholesteric liquid crystals (Ref. 39). A mixture of 90% cholesteryl nonanoate and 10% cholesteryl myristate covering the entire color range from red to purple in 0.2°C (from 72.6°C to 72.8°C) was used. The rotor blades were painted with india ink to provide a uniform black coating. It had been determined that subsurface flaws were best revealed in transient thermal conditions. Several different methods were tried with the most success achieved by heating from beneath and cooling the surface to be examined. The surface of a rotor blade is not flat, so in order to achieve some uniformity, the bottom was heated with a 500-watt photoflood lamp, and the top cooled by a stream of room temperature air. Flaw indications frequently existed for only a few seconds in each heating/cooling cycle. Heat flow in the liquid crystal from uneven spreading may cause an irregular color pattern when no subsurface anomaly exists, so care was taken to obtain uniform layers. Both rotor blades had voids which were detectable using the liquid crystals. Tests of damage caused by striking foreign objects and crushing were also made. Cholesteric liquid crystals were shown to provide a simple, straight-forward NDE method. Little training was needed to conduct tests or to interpret the results. Liquid crystals used temperatures low enough to be safe. One conclusion was that use of sheets of encapsulated liquid crystals would have enhanced their use.

Pontello of the Naval Air Propulsion Test Center has reported a method using liquid crystals for 100% inspection of coalescer elements (fuel filters) (Ref. 40). Flaws such as voids, split seams, end cap leaks, and cracks, as well as material imperfections and epoxy- filled voids were detected. The Navy had severe problems with coalescers, and costly damage to fuel systems had been traced to them. Figure 29 shows the coalescer element which was used to filter solids and remove water from jet fuels.

A test facility was developed to use liquid crystal inspection. Figure 30 is a schematic of that system. The coalescer was placed in a cylindrical aluminum housing consisting of two end caps and held together by three aluminum ribs. Around these ribs was wrapped a 0.00635 mm (0.00025 in.) thick sheet of mylar film. The coalescer was exposed to the inner surface of the film. The circle of colors appearing over a flaw was larger than the width of the ribs, so problems with obscured areas were avoided. Pre-blackened liquid crystals were sprayed onto outer surface of the Mylar, thus eliminating direct contact of the liquid crystals with the coalescer. Heated air at 82°C (180°F) was circulated through the coalescer against the uncoated side of the Mylar to ensure rapid drying and even distribution of the liquid crystals, promote adherence of the crystals, and ensure complete solvent evaporation. The preheating of the crystals resulted in an increase in the brilliance of colors. The same liquid crystals were used repeatedly over several weeks. The Mylar film was cleaned of liquid crystals when necessary by wiping with petroleum ether.

Compressed air was supplied through a pressure regulator. The inlet air heating element at the bottom of the coalescer housing was controlled by a rheostat. The rheostat controlled the temperature to correspond to the operating range of the crystals and temperature and pressure were measured at the inlet to the coalescer. After passing through the coalescer, the air flowed through the space between the coalescer and the Mylar films, and out through the top of the unit. All nondestructive tests were done with the element in a stationary position. A mirror at the rear of the coalescer allowed observation of all flaws from one position.

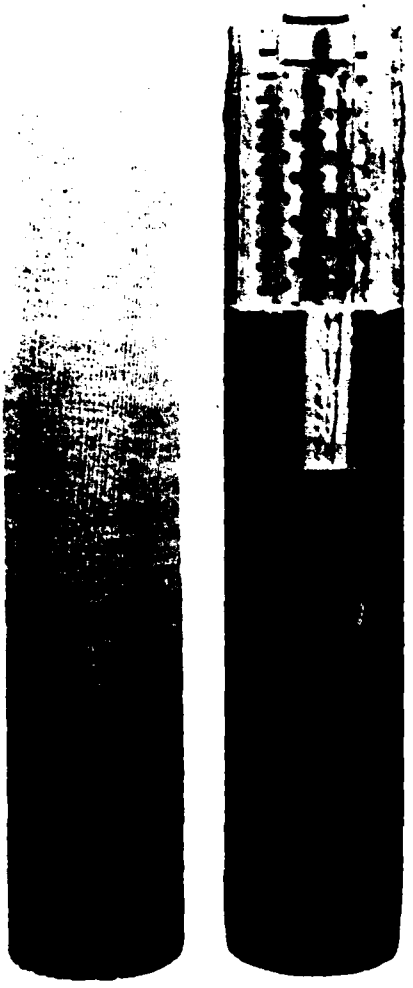

Figure 29. Filter Coalescer Element (From Ref. 40, Photograph Used by Permission of The American Society of Mechanical Engineers, N Y)

Figure 31 shows test results for voids having 8.5, 1.6, and 1.2 mm (1/8, 1/16, and 3/64 in.) diameters. It is clear that liquid crystals are good materials for this testing requirement.

Pontello later reported additional work on testing of coalescers in which encapsulated liquid crystals were used (Ref. 41). Tests for flaws obscured by the cotton sock were made using a mirror for observation. Two coalescers were tested. One contained two 1.2 mm (3/64 in.) voids inserted at angles of 60 and 45°. It is normally difficult to detect seam splits because they are disguised by the line made by the seam. Other types of flaws detected were voids with diameters of 3.2 through 1.2 mm (1/8 through 3/64 in.), voids as small as 0.4 mm (1/64 in.), and material imperfections caused by variations in the thickness of the fiber layers. Also detected

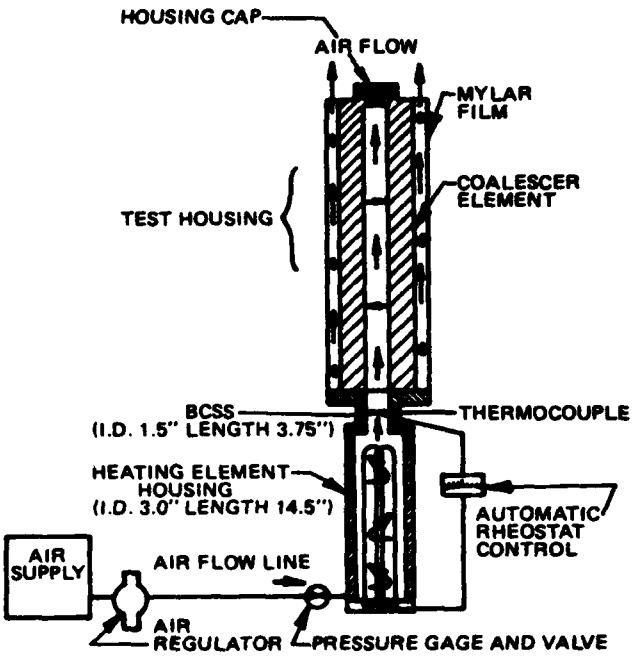

Figure 30. Schematic of Test System for Using Liquid Crystals to Test Coalescers (From Ref. 40, Reproduced by Permission of The American Society of Mechanical Engineers, N Y)

were a cracked end cap, and a separated end cap seal, two of the most common defects in coalescer elements.

A limited investigation of the application of liquid crystals to tire inspection was conducted by Lavery (Ref. 42). Flat rubber/cord samples were coated with liquid crystals to evaluate their use in detection of disbonds and to determine the effect of rubber on liquid crystals. Heat was applied behind the sample or in front of the sample and disbonds were easily detected, but contamination of the liquid crystal occurred. One possible remedy is to use encapsulated liquid crystals. Another is to provide an impermeable membrane between the rubber and liquid crystal. It was planned to routinely use encapsulated liquid crystals for future inspection during dynamic tire tests as a backup to infrared inspection.

Liquid crystals have been used to test aircraft windshield heaters (Ref. 22). They were applied to the outer surface, after which current was passed through the electrical heating elements and a known amount of power was applied. Isotherm plots as a function of time were made on a Mylar sheet laid over the liquid crystals. Figure 32 shows the isothermal plot of a Boeing 707 windshield. The areas that had reached 33°C at given times are shown. It is determined if a heating element is performing satisfactorily by comparison to standard curves. Liquid crystals appeared to respond more rapid-

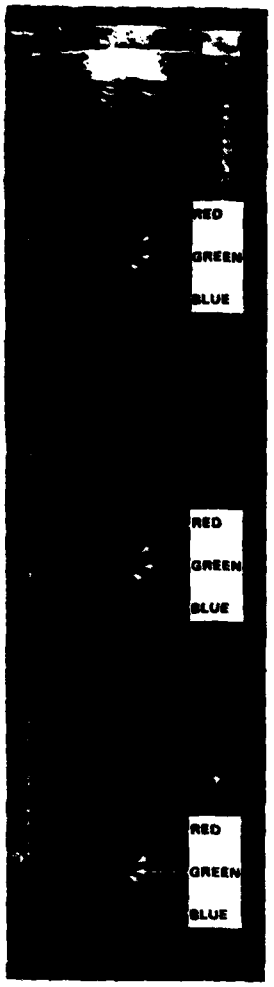

1/8" diameter void

1/16" diameter void

3/64" diameter void

Figure 31. Detection of Coalescer Flaws Using Liquid Crystals (From Ref. 40, Photograph Used by Permission of The American Society of Mechanical Engineers, N Y)

ly than previously used indicators, were easier to use, worked at lower temperatures, and were reversible and reusable.

6. Flaw Testing With Nematics

A technique using the effect of electric fields to produce dynamic scattering modes in nematic liquid crystals for nondestructive examination of lacquered metal surfaces has been investigated by Farr, Keen, and Pettitt (Ref. 43). This technique is an adaptation of a method previously reported by Keen (Ref. 44) for integrated circuits, which will be discussed in a subsequent section. This investigation was initiated specifically to detect pinholes and imperfections in the lacquer applied to tin-plate used for manufacture of cans.

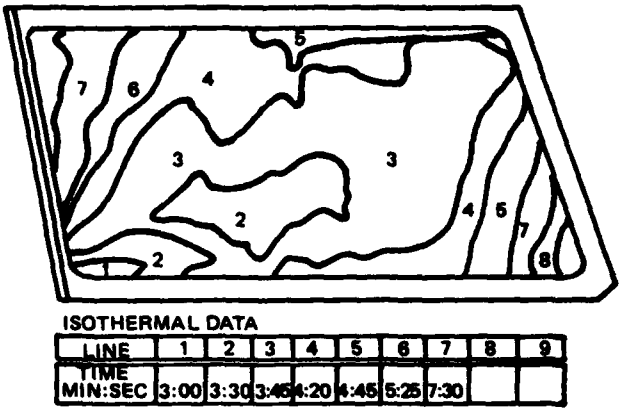

Figure 32. Aircraft Windshield Heating Pattern [Initial Light Scattering at 33°C] (From Ref. 22, Reproduced by Permission of Optical Society of America, Washington, D C)

Figure 33 illustrates the experimental arrangement. The cell was positioned under an optical microscope and the liquid crystal layer or the metal surface beneath it was illuminated through the cover glass. Both 4-*methoxy-4-n-butylbenzylideneaniline* (MBBA) having a range of 21-47°C, and a proprietary 10-47°C liquid crystal were used. (The temperatures in this case refer to the range of liquid crystallinity and not a color range.) A d.c. voltage across the cell was controlled by a potentiometer circuit. The voltage was increased to threshold. When the liquid crystal threshold was exceeded, turbulence was seen, the turbulence resulting in a dynamic display. Higher voltages, typically 15-20V for regions of complete absence of lacquer, were required to produce turbulent displays on the lacquered tin-plate than on semiconductor devices. (See the later discussion of Keen's work as reported in Ref. 44). The liquid crystal usually was removed with alcohol immediately after tests since some softening of the lacquer occurred if the liquid crystals were left on for several hours.

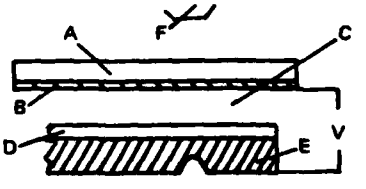

Figure 33. The Experimental Arrangement. A. Microscope Cover Slide, B. Tin Oxide Layer, C. Nematic Liquid Crystal, D. Lacquer Film, E. Tin Plated Steel Sheet, F. Microscope Objective, V. Stabilised Voltage Source (From Ref. 43, Reproduced by Permission of Elsevier Sequoia S.A., Lausanne, Switzerland)

Figures 34 and 35 show the results of tests on the contoured ends of "pop top" cans. Since the lacquered plate is subjected to deformation during manufacture, inspection of the survival of lacquer films was desirable. Such films must also withstand abrasion and scratching. Scratches made by a diamond stylus under calibrated loading have been studied with liquid crystals. Defects in insulating layers on metals and on electroplating, etc. are often detected by deposition of copper. Some disadvantages are (1) it will only deposit on complete punctures, (2) there is no quantitative scale, (3) microscopes must be used, and (4) the method is destructive. Liquid crystals alleviate or eliminate all these.

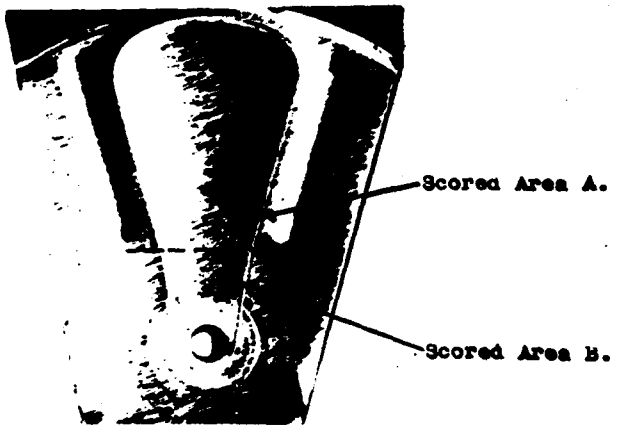

Figure 34. The Lacquered Underside of Part of a Scored Aluminum Can Top Indicating the Deformed Regions shown in Fig. 35 (From Ref. 43, Photograph Used by Permission of Elsevier Sequoia, S.A., Lausanne, Switzerland)

7. The Nondestructive Use of Liquid Crystals in Fatigue, Flow, and Fracture Tests

Because of their sensitivity and rapid response to small temperature variations, cholesteric liquid crystals were applied by Woodmansee to detection of thermal conversion of mechanical energy during deformation (Ref. 22). Thermal gradients created by strain concentrations were detected on two types of specimens. The tip of a growing fatigue crack was indicated by an area of higher temperature corresponding to the expected plastic region. For sheet metal tensile tests, the beginning of plastic instability and its location were seen as a local change in color, and thus, an increase in temperature, before necking could be detected.

Just before rupture, transitory, flickering changes were observed. It was assumed that these thermal transients were associated with unstable plastic flow. An aluminum alloy (5456 in the H321 condition) that exhibits prominent strain irregularities above its yield point was therefore tested. Liquid crystals indicated thermal changes corresponding to the load-strain curve, thus verifying the assumption. At the same time, Luder bands or stretcher strains began appearing during stretch forming large panels of one of the samples, 2024-T3, an unusual problem with this material. Luder bands are caused by unstable plastic flow and appear abruptly as local bands of thinning. The inability to detect or control the responsible strain irregularities in uniaxial tensile specimens made laboratory tests difficult, but liquid crystals gave visual evidence of the formation, location, and orientation of the Luder bands.

Forman reported the use of cholesteric liquid crystals to monitor strain heat for locating areas of stress and potential fractures in metals (Ref. 34). The use of the usual strain measuring devices and instrumentation for sensing temperature to monitor heat and strain is limited by the necessity of predicting the location of defects prior to testing. A liquid crystal blend, which could be applied over a large area, was used and alleviated the need to predict locations of defects. Various rates of applying stress were investigated to determine the best conditions for observing the color changes. A blue area around the hole in the center of the tensile specimen revealed the area of concentrated stress where more heat is produced. Red areas designated lower temperatures (or less stress). Thermal gradients could easily be seen and Luder lines were observed.

Singleton has reported the use of cholesteric liquid crystals to monitor the temperature generated in bars under tensile test to fracture (Ref. 45). Previous reports had identified local cooling of these bars in similar test situations and the object of this work was to verify or reject this finding. The liquid crystals were selected to function in the range to be found if the previous report was correct. However, no cooling was found; in fact, intense heating occurred and consequently, the liquid crystals were heated out of their operational range. They did, however, indicate that heating rather than cooling, occurred. The liquid crystal data was recorded by use of 8 mm color motion picture film.

8. The Use of Liquid Crystals in Fluid Flow Measurements

Klein and Margozzi, in 1969, reported the use of coatings of cholesteric liquid crystals sensitive to shear, rather than temperature, to measure local skin friction in aerodynamic testing (Ref. 46). Scattering wavelength changes were used as the indicator. The criteria for selecting a liquid crystal mixture were (1) shear sensitivity, (2) temperature insensitivity, and (3) chemical stability. A mixture containing proportions of four liquid crystals was used. A calibration of shear versus wavelength was obtained and a static (shear) calibration was made to measure the effects of temperature, pressure, and viewing angle. Feasibility was shown.

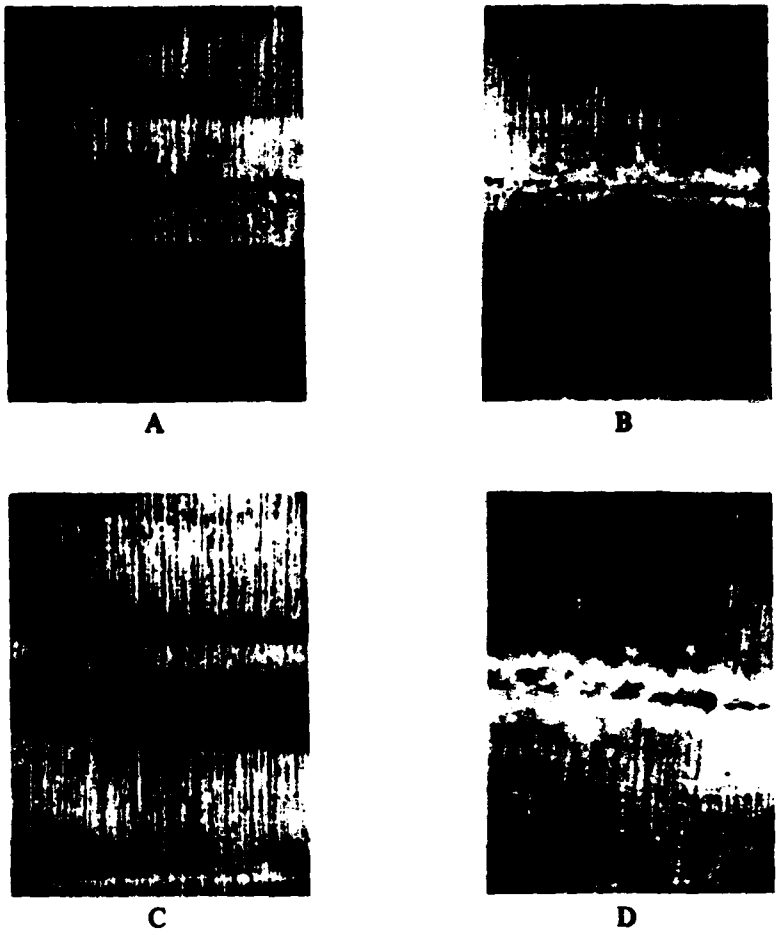

Figure 35. Liquid Crystal Examination of Lacquer After Deformation, Using the Nematic mbba at 23°. Magnification X 50. [a] Scored Area A, Bright Field Illumination, Applied Voltage 0 V; [b] Scored Area A, Dark Field Illumination, Applied Voltage 400 V; [c] Scored Area B, Bright Field Illumination, Applied Voltage 0 V; [d] Scored Area B, Dark Field Illumination, Applied Voltage 400 V (From Ref. 43, Photograph Used by Permission of Elsevier Sequoia, S.A., Lausanne, Switzerland)

Liquid crystals have been used by Knox to investigate pressure distributions on an 80° swept tetrahedron body at Mach 5 and angles of attack of 0, 5, and 10° (Ref. 47). The liquid crystal technique was under investigation to evaluate its potential for visual detection of boundary layer transition. In these tests the results were inconclusive because the liquid crystals were incorrectly applied and protected.

Real-time visualization of unsteady boundary layers was reported by Lemberg (Ref. 48). This was an extension of the work of Klein (Ref. 49) who investigated steady-state layers. For this analysis the time response characteristics are of prime importance. Factors affecting time response are (1) film thickness, (2) material (substrate) thickness, (3) an infinite thickness of a second material, and (4) heat transfer coefficients. Maximum response, according to analysis, is achieved when the film thickness is large enough to give good color intensity (10-40 μm) and when the substrate has low thermal conductivity and a thickness which is large compared with the maximum frequency of change multipled by the heat capacity of the liquid crystal and divided by the liquid crystal thermal conductivity. Since the thermal time constant of liquid crystals is at best 4 Hz for unit input and 500 Hz for an input ten times larger, the smallest observable temperature change for visual detec-

tion is about one-third the temperature range required to go from red through green to blue. For example, if this range were 1°C, then changes of 0.3°C could be readily discerned.

9. Acoustic Detection and Imaging

The temperature of materials which absorb energy, in this case, acoustic energy, rises as the energy is absorbed. Therefore, if a cholesteric liquid crystal is applied to a sound absorber, the ultrasonic field distribution can be visualized as a colored pattern when placed in the ultrasonic field. This effect could also be used to map the vibrational modes of mechanical resonators by appropriate coupling between the resonator and the absorber to which the liquid crystal has been applied. Thus, liquid crystals can be used directly in NDE as ultrasonic detectors and mappers or to calibrate and map transducers which would be used.

Sproat and Cohen report that experiments based on direct excitation of cholesteric crystals by ultrasonic energy gave negative results, and that, consequently, they adopted the approach of using an intermediate conversion of the ultrasonic energy to heat via an ultrasonic absorber (Ref. 50). The experimental set-up is shown in Figure 36. The water immersion tank used for acoustic energy transmission also provided a means to bias detector temperature just below the onset of color transitions. A 1 MHz source was used and had an unfocused main lobe intensity of approximately 1 MW/m² (100 W/cm²). Exposure durations of 1 to 10 seconds were required and produced results like that of Figure 37. If the temperature of the water was properly maintained, the limit on resolution for these experiments was determined by ultrasonic diffraction rather than the detector.

Temperature sensitive light scattering by cholesteric liquid crystals has been used by Cook and Werchan for mapping intensity distributions of the near-field of

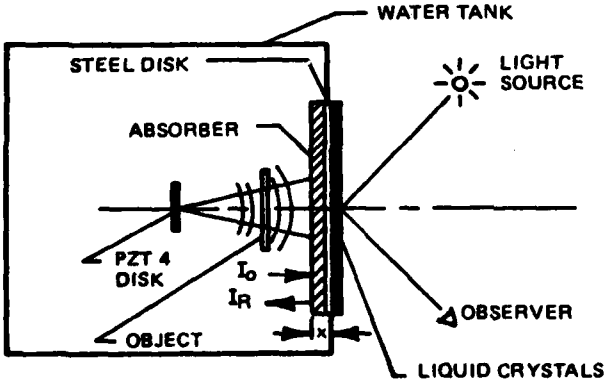

Figure 36. Schematic of the Acoustographic (AGIS) Imaging System (From Ref. 50, Reproduced by Permission of The American Society for Nondestructive Testing, Inc., Columbus, OH)

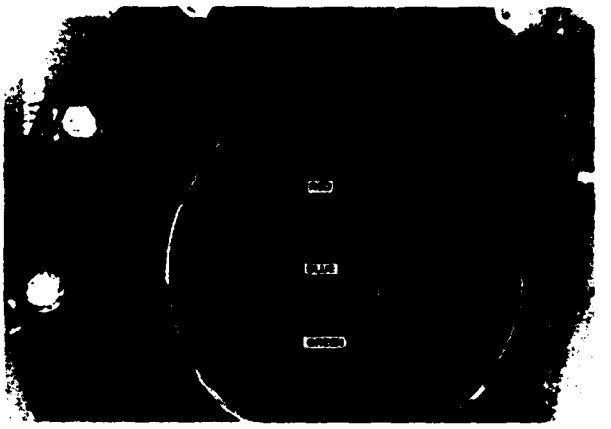

Figure 37. Cholesteric Liquid Crystal Imaging of Ultrasodic Energy Via an Intermediate Conversion to Heat (From Ref. 50, Photograph Used by Permission of The American Society for Nondestructive Testing, Inc., Columbus, OH)

ultrasonic transducers (Ref. 51). Full color maps gave a spatially continuous display of the ultrasonic intensity in a plane. A sound field established a thermal equilibrium in 3 to 5 seconds and lateral heat flow erased the display after approximately 10 seconds.

Liquid crystals were used by Maple to observe transient and steady state patterns of AN/SQS-26 transducers (Ref. 52). The transient temperature range to be covered was determined by running the transducers and making spot temperature measurements with thermocouples for a period of one hour. The range was determined to be approximately 18 to 30°C (65 to 86°F). A 10% liquid crystal solution in chloroform was used. Calibration gave the following transition temperatures:

black to red 18.3°C (65°F)
red to yellow 21.1°C (70°F)
yellow to green 22.2°C (72°F)
green to blue 24.4°C (76°F)
blue to violet 25.5°C (78°F)
violet to black 30°C (86°F)

A floodlamp was used to illuminate the transducer and was switched on momentarily for each photograph so that additional heating could be avoided.

Also with thermocouples, the steady state temperature of the head area was determined to vary between 57.2-64.4°C (135-148°F) and the stock between 40.0-62.8°C (104-145°F). Calibration for chloroform diluted liquid crystals is shown:

Head-Mass Formulation

black to red 57.2°C (135°F)
red to yellow 58.3°C (137°F)
yellow to green 58.9°C (138°F)
green to blue 60.0°C (140°F)

blue to violet 62.2 °C (144 °F)
violet to black 64.4 °C (148 °F)

Ceramic-Stack Formulation

black to red 40.0 °C (104 °F)
red to yellow 45.0 °C (113 °F)
yellow to green 46.1 °C (115 °F)
green to blue 48.3 °C (119 °F)
blue to violet 51.7 °C (125 °F)
violet to black 62.8 °C (145 °F)

Test results are shown as isotherms in Figure 38. This

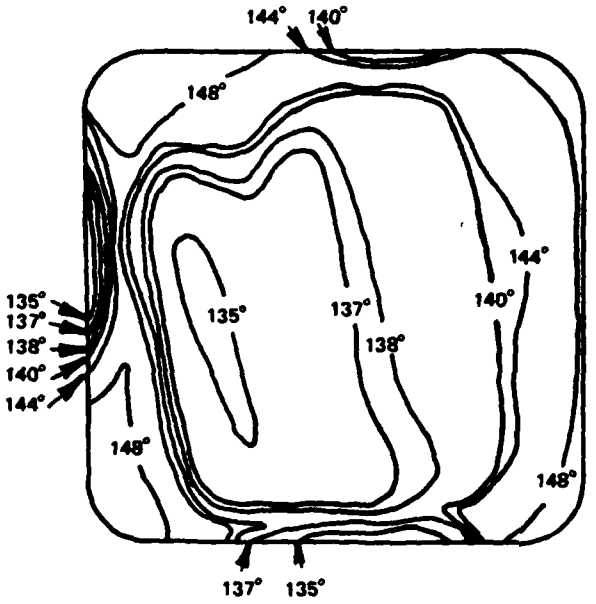

Figure 38. Thermal Mapping of AN/SQS-26 Transducers (From Ref. 52, Reproduced by Permission of Office of Naval Research, Washington, D C)

study showed that cholesteric liquid crystals are valid, low-cost materials for observing surface thermal patterns.

Kagawa, Hatakeyama, and Tanaka used the arrangement in Figure 39 to investigate ultrasonic detection using cholesteric liquid crystals (Ref. 53). A 35 °C constant temperature was maintained using an electronic temperature controller which held the bath to within 0.2 °C over its entire volume and throughout the experiment. Sound absorbers were used on the bath wall to prevent multiple-reflections. The liquid crystal plate detector was in front of the radiator and parallel to it, as shown. A 100 μm thick polyester sheet was painted with temperature sensitive encapsulated cholesteric liquid crystal on one surface and black color on the other, and had the color-temperature characteristic shown in Figure 40. The sheet was glued on a 10 cm × 10 cm × 1 mm thick PVC plate to improve sound absorption. Electron grease was applied on the surfaces to prevent water contamination. Figures 41 and 42 illustrate the

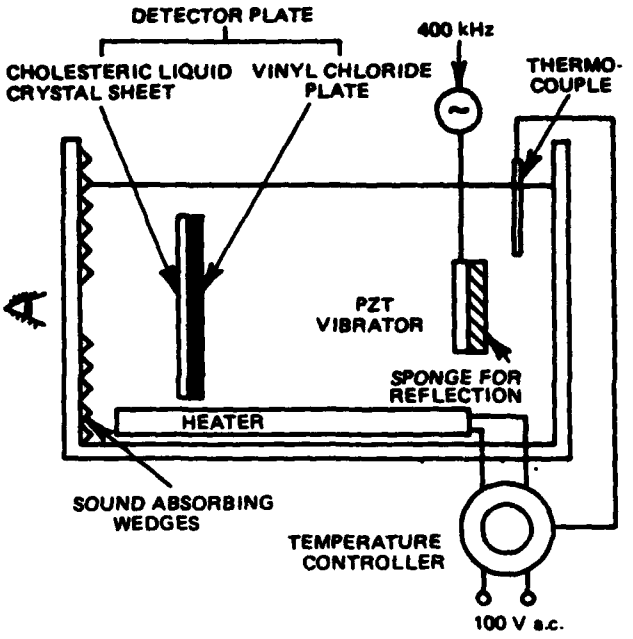

Figure 39. Experimental Arrangement for the Detection of Ultrasonic Field by Cholesteric Liquid Crystal (From Ref. 53, Reproduced by Permission of Academic Press Inc. [London] Ltd.)

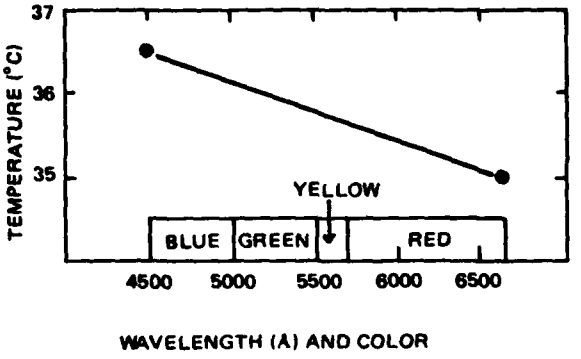

Figure 40. Temperature Versus Produced Color of the Cholesteric Liquid Crystal Employed in the Experiment (From Ref. 53, Reproduced by Permission of Academic Press Inc. [London] Ltd.)

results of near-field mapping using the cholesteric material. Demonstration of the mapping of vibrational modes was done with a hand-held PZT, 1 cm × 6 cm × 0.5 cm thick, which vibrates in-plane as shown in Figure 43 (Ref. 53). The cholesteric liquid crystal sheet was loosely coupled to the vibrator surface with electron grease. Heat was caused by relative motion between the vibrating surface and the still sheet, and the modal pattern was shown as color change. The ambient temperature was kept constant. In Figure 44 the modal

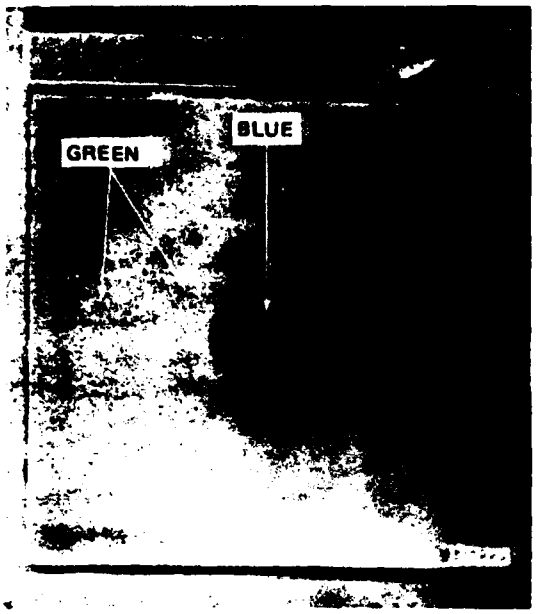

Figure 41. Ultrasonic Near-Field Pattern Produced on the Cholesteric Liquid Crystal Detective Plate for a Circular Vibrator Radiator. Diameter: 5 cm; Distance: 4·5 cm; at 400 kHz (From Ref. 53, Photograph Used by Permission of Academic Press Inc. [London] Ltd.)

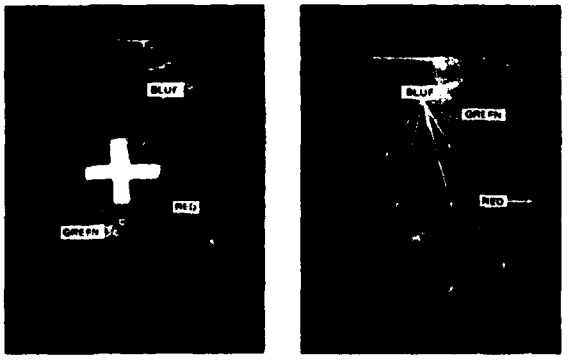

A B

Figure 42. Simple Ultrasonic Camera. [a] Cross-Shaped Object Made of Foamed Polystyrene; [b] Shadow Image on the Rear Face of the Cholesteric Liquid Crystal Detective Plate (From Ref. 53, Photograph Used by Permission of Academic Press Inc. [London] Ltd.)

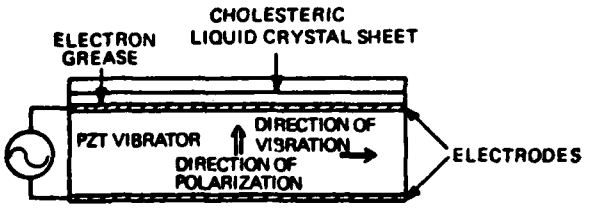

Figure 43. Arrangement for the Detection of Vibrational Modes of a Vibrator by Cholesteric Liquid Crystal (From Ref. 53, Reproduced by Permission of Academic Press Inc. [London] Ltd.)

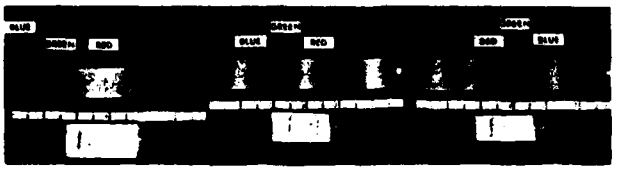

A

B

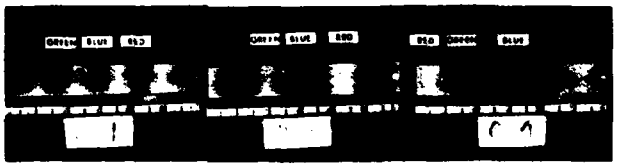

C

Figure 44. Modal Patterns of a PZT Vibrator as Detected by Liquid Crystals (From Ref. 53, Photograph Used by Permission of Academic Press Inc. [London] Ltd.)

patterns of a PZT vibrator as detected by liquid crystals are shown.

Figure 45 (Ref. 54) illustrates the device used by Manaranche and Henry for experiments on detection of an ultrasonic beam by cholesteric liquid crystals (Ref. 54). The cylindrical tank was filled with water, the temperature of which was controlled by a thermostat. At one end was a watertight circular window made of 100μm thick polyethylene. The external side of the diaphragm was blackened and then covered with an even layer of cholesteric liquid crystals. A mixture of two proprietary products, the resulting sensitivity range of which was 38.5-40.5°C, was used. The bath temperature was adjusted by the thermostat, to the lower temperature of the stability range at which the diaphragm was dark red. The transducer to be tested was then placed on the axis of the cylinder so as to direct the ultrasonic beam towards the center of the window. The transverse ultrasonic fields of four different transducers were mapped. Figure 46 shows the spot obtained at 117 mm with a 120 mm focal length probe at 3 MHz. It was concluded that this technique allows the

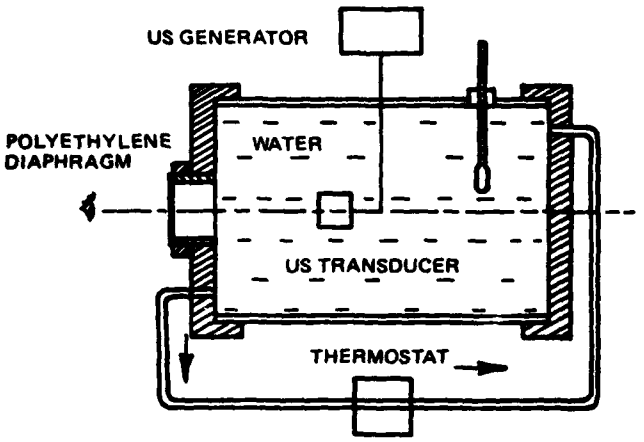

Figure 45. Device for the Detection of Ultrasonic Beam by Liquid Crystals (From Ref. 54, Reproduced by Permission of British Institute of Nondestructive Testing, Southend-on-Sea Essex, England)

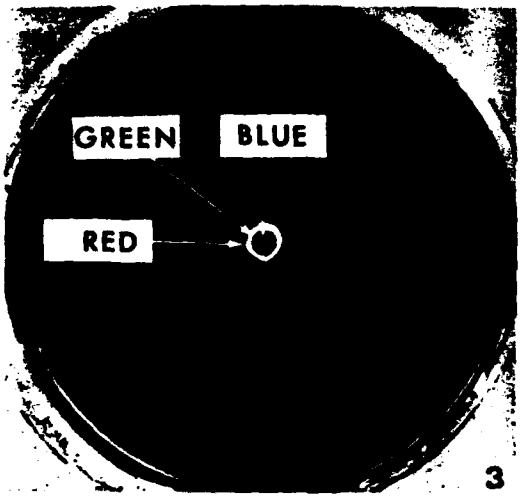

Figure 46. Spot Obtained at 117 mm with a 120 mm Focal Length Probe [3 MHz] (From Ref. 54, Photograph Used by Permission of British Institute of Nondestructive Testing, Southend-on-Sea Essex, England)

obtaining of detailed and precise knowledge of the performance of ultrasonic transducers with an inexpensive and simple device.

Fourney, Auth, Intlekofer, and Kobayashi report development of acoustical holography for nondestructive investigation of surface flaws using a cholesteric liquid crystal area detector as the read-out device (Ref. 55). Liquid crystal area detectors were shown feasible and had a resolution limit in excess of 10 lines/mm, an order of magnitude improvement over other techniques, such as the liquid "ripple tank." The resolution was not fully used because of (1) scattering of the ultrasonic wave by grain boundaries, (2) near-field distortions of the ultrasonic transducers, (3) an incomplete knowledge of the interaction of the ultrasonic waves and the liquid crystal, and others. Cholesteric liquid crystal area detectors for acoustical holography have some disadvantages, such as low sensitivity and small dynamic range. However, they do have high resolution and were shown to be compatible with the use of acoustical holography in solids.

The acoustic detection mechanism for nematic liquid crystals is a direct interaction with the birefringence. The effects of the acoustic energy are very similar to those experienced with an electric field which produces dynamic scattering. Electric field biasing overcomes the effects of surface forces caused by plates and causes the liquid crystal to be more sensitive to the acoustic energy as illustrated in Figure 47 (Ref. 56).

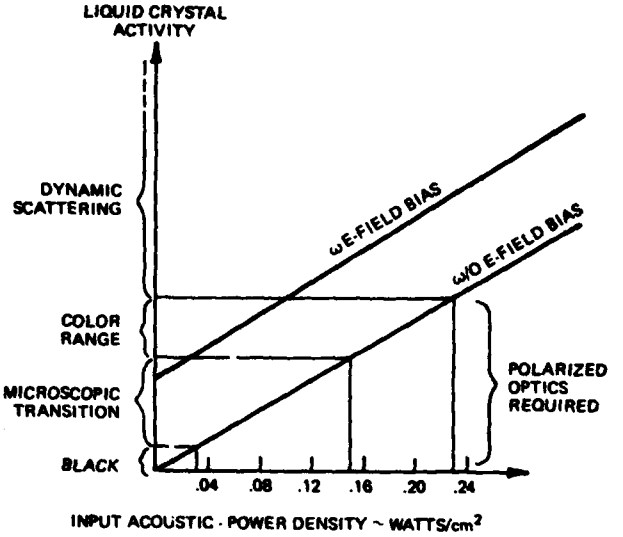

Figure 47. Activity of Liquid Crystal Cell in Response to 10 MHz Ultrasound With and Without 3.75 Volt d.c. Bias. (From Ref. 56, Reproduced by Permission of Gordon and Breach, Science Publishers, Inc., N Y)

Mailer, Likins, Golis, and McMaster fabricated a nematic liquid crystal cell to evaluate the capability of the material to detect and display ultrasonic images (Ref. 56). The cell was made of two glass plates 100 × 90 × 3.175 mm (4 × 3.5. × 0.125 in.) thick separated by 38.1 μm (0.0015 in.) mylar spacers and was filled with a normally aligned nematic crystal. The cell was evaluated as shown in Figures 48 and 49, which show transmission and reflection experiments respectively. In the reflection experiment, the bottom plate had a reflective coating to reflect light to the observer. A "collimated" 30 watt light source was used. Ultrasonic energy was produced by a transducer at 10 MHz.

An arrangement similar to that for their previously discussed experiments with cholesteric liquid crystals was used by Kagawa, Hatakeyama, and Tanaka to

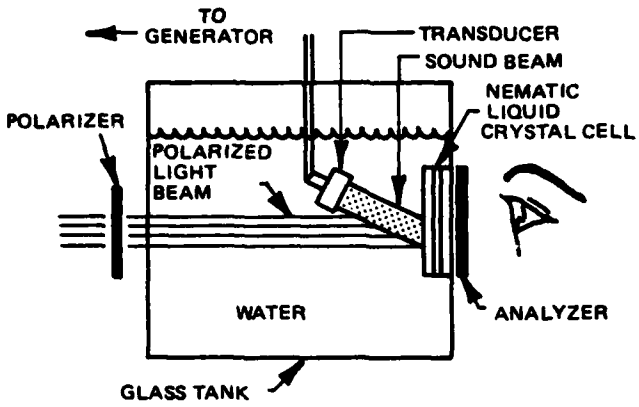

Figure 48. Schematic Representation of Experimental Configuration Used to Evaluate Nematic Liquid Crystal Cells in the Optical Transmission Mode. Polarizer and Analyzer are Adjusted for Extinction in the Absence of Ultrasound. (From Ref. 56, Reproduced by Permission of Gordon and Breach, Science Publishers, Inc., N Y)

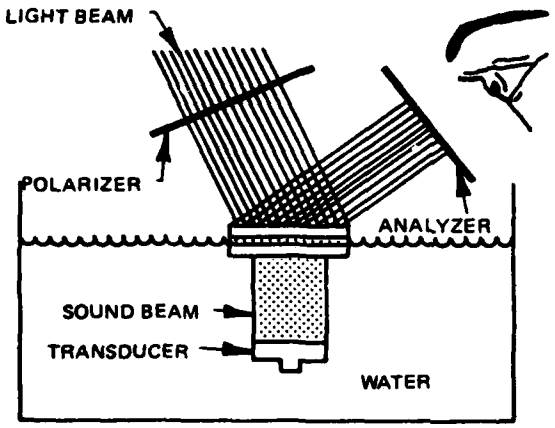

Figure 49. Schematic Representation of Experimental Configuration Used to Evaluate Nematic Liquid Crystal Cells in the Optical-Reflective Mode. Polarizer and Analyzer are Adjusted for Extinction in the Absence of Ultrasound. (From Ref. 56, Reproduced by Permission of Gordon and Breach, Science Publishers, Inc., N Y)

investigate nematic materials (Ref. 53). A polarizer-analyzer pair was added, and water temperature was not so critical. The detector plate was a nematic liquid crystal layer sandwiched between a pair of glass plates with a conductive, transparent coating used as an electrode. The plate was 10 × 10 cm². A thin air space was provided by inserting a 10 μm polyester spacer between the plates. MBBA liquid crystal was infused by capillary action. Two kinds of treatment provided molecular orientation perpendicular to the plates: (1) application of lecithin to the substrate surfaces and (2) doping the MBBA with a small amount of cetyltrimethylammonium bromide. Figure 50 shows results for no applied voltage and the enhancement for an applied voltage of 7.6 volts. The vibrator from the cholesteric

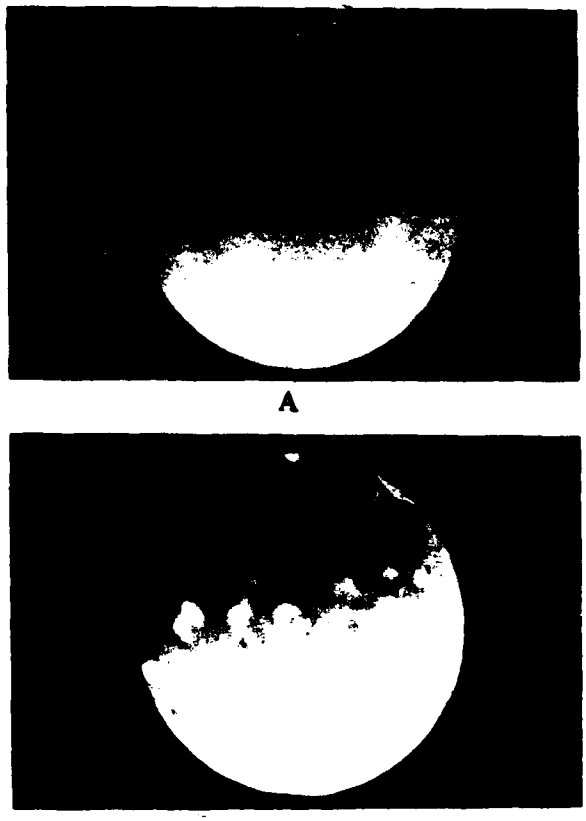

A

B

Figure 50. Sound Pressure Sensitivity is Found Increased with Electric Field Superposed, While the Sound Intensity is Kept Constant [distance: 4·5 cm]. [a] Applied Voltage: 0 V; [b] Applied Voltage: 7.6 V (From Ref. 53, Photograph Used by Permission of Academic Press Inc. [London] Ltd.)

experiment was used to demonstrate modal vibration mapping. A pair of thin (100 μm) wire spacers was placed on the vibrator surface and covered by a thin glass plate. MBBA was infused into the space. When the vibrator vibrated in-plane, shearing strain developed from the relative motion between the glass plate and the vibrating surface. Under polarized lighting a vibrational mode pattern could be seen, even by the naked eye, when the dynamic scattering mode was excited. Figure 51 shows the modal patterns of a PZT vibrator obtained with a nematic layer.

Recently, visualization of elastic deformation using nematic liquid crystals which were not in the dynamic scattering mode has been demonstrated by Scudieri, Verginelli, and Ferrarri (Ref. 57). Hydrodynamic instabilities—in birefringence—which require less mechanical power were observed. Normal deformation modes of a glass plate driven piezoelectrically were observed using the set up shown in Figure 52. Figure 53 shows the results for a 75 μm thick sample driven at 8.64kHz.

B. Use of Liquid Crystals to Examine Electronic Components and Assemblies

1. Circuit Boards and Assemblies

Woodmansee reported the use of cholesteric liquid crystals to locate shorts in circuit boards for a Minuteman electronic control system (Ref. 22). Resistance measurements readily reveal the existence of interlayer shorts in multilayer circuit boards, but do not locate them. In the case reported, location of the short

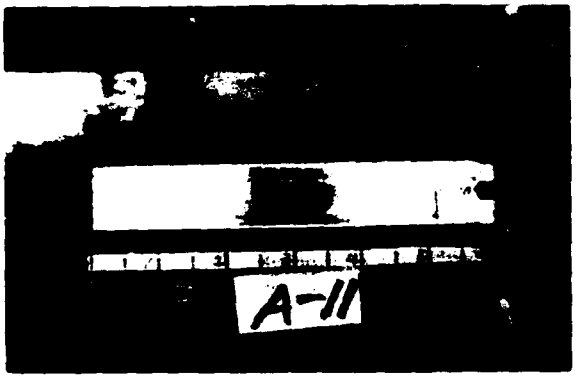

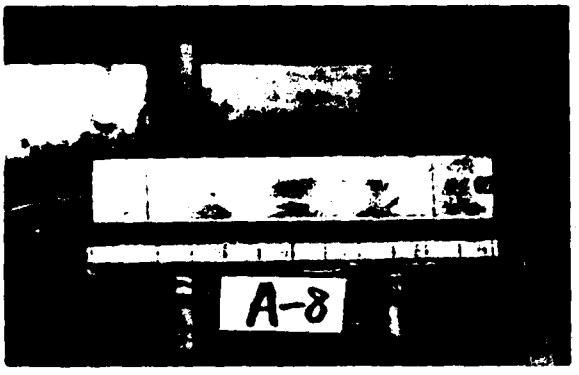

Figure 51. Modal Patterns of a PZT Vibrator by Means of the Nematic Liquid Crystal Layer. Brighter Regions are Due to the Dynamic Scattering Mode (DSM) (From Ref. 53, Photograph Used by Permission of Academic Press Inc. [London] Ltd.)

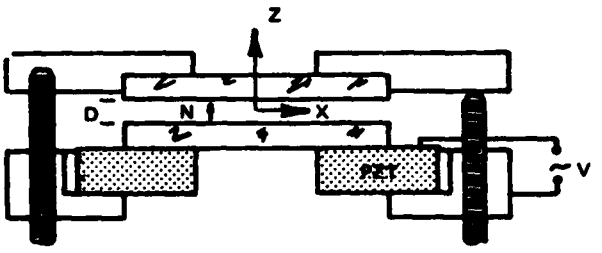

Figure 52. Sketch of Cell Used for Visualization of Elastic Deformation at Levels Below the Threshold for Dynamic Scattering (From Ref. 57, Reproduced by Permission of Springer-Verlag, Publisher, N Y)

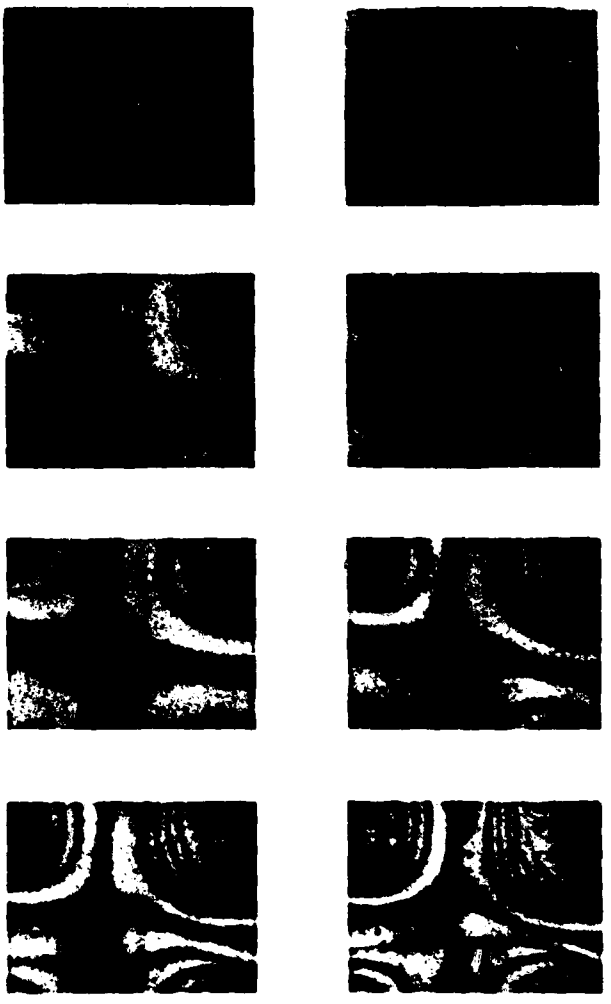

Figure 53. Visualization of Elastic Deformation with Nematic Liquid Crystals by Observation of Hydrodynamic Instabilities in Birefringence (From Ref. 57, Photograph Used by Permission of Springer-Verlag, Publisher, N Y)

was not possible even after careful examination of radiographs. The use of current flow through the shorted layers with liquid crystals applied to one surface of the board located the short quickly. A liquid crystal mixed with tempera black paint, to eliminate the need for a black background paint, was used. A 25-50 μm (1-2 mil) diameter metallic particle was found to be responsible.

Circuit boards (flip-flop circuits) were tested by Forman using nonanoate butyrate, which has its active range at room temperature (Ref. 34). Ink was used to provide a dark background. As the circuit began operating, and for equal applied voltages, low value resistors were distinguishable from high valued ones by a faster rate of color changes caused by higher currents. Open components did not change color at all as there was no current to produce heat. Hot spots or high resistance printed circuits produced unusual color patterns.

Multi-layer circuit board interconnectors were investigated by Woodmansee using coatings of liquid crystals (Ref. 30). As current passed through the circuits, high resistance connections could be identified. One connection had a resistance of 11.6 milliohm and was distinguishable from those having resistances near the average of 4 milliohm.

Marto and Kelleher modeled and conducted measurements of the air flow through equipment racks designed for circuit boards containing integrated circuits and LSI devices, to locate hot spots on boards, and to provide thermal performance data on fiberglass/epoxy and aluminum core circuit boards under the packaging conditions in the racks (Ref. 58). Liquid crystal thermography was used to investigate convective heat transfer, giving a direct visualization of hot spots. Both a uniformly heated smooth board and a uniformly heated board with nine passive resistors attached were used. The uniformly heated board showed hot spots caused by the convective air flow only and minimized temperature variations caused by nonuniform distribution of heat sources (such as current carrying resistors). A special board was made by attaching Temsheet (stiff, black, porous paper impregnated with carbon) to a smooth fiberglass-epoxy board, uniform electrical resistivity being provided by the carbon. Electrodes were attached to opposite edges of the Temsheet and a current passed through it to generate uniform heat. Liquid crystals having a color range from 59-62°C were used. This board was placed in the middle of three sets of board guides between two dummy boards, one of which was made from Plexiglas to allow viewing of the liquid crystal board.

For a subsequent set of experiments, nine ceramic cased resistors were glued directly to the Temsheet board to serve as flow obstructions. The influence of the resistors and the flow around them on the surface temperature of the heated Temsheet board was observed. Flow rates from 330 to 1580 $cm^{3/s}$ (0.7 CFM to 3.335 CFM) were used for the Temsheet board. Power was varied from 12 to 24 watts. Figure 54 shows one set of isotherms which was obtained.

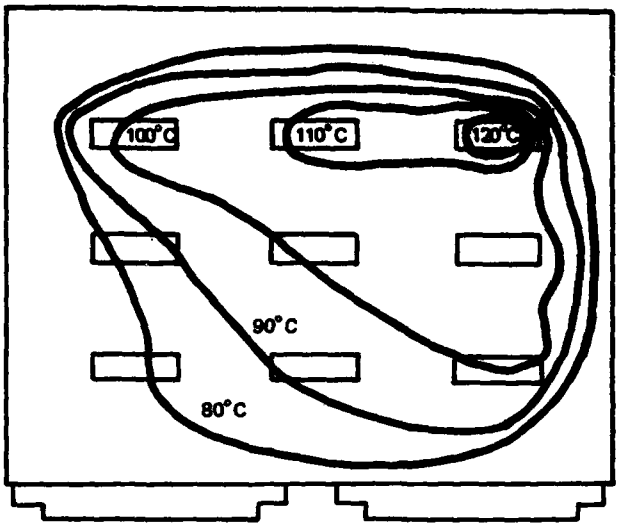

Figure 54. Schematic Representation of Isotherms on the Fiberglass/Epoxy Board, 0.76 CFM/Board, 13.0 Watts/Board (From Ref. 58, Reproduced by Permission of Research Library, Naval Postgraduate School, CA)

2. Circuit Components

Figure 55 shows a temperature distribution pattern on five 500 ohm ±1% resistors as determined by Woodmansee (Ref. 30). The applied voltage was approximately 10 volts. As can be seen, the surface temperatures vary considerably. At the time of these tests no correspondence between the variations in surface temperature and resistor properties had been determined, but there was speculation that nonuniformity meant shorter life expectancies.

Thin film Al-AlO_2-Al capacitors having a 150 nm thick dielectric film were inspected by Lescinsky and Fridrich using MBBA (Ref. 59). The capacitor was covered by a drop of liquid crystal and the structure observed upon application of 18 volts d.c.. Two types of defects were observed: (1) those which remained visible even after removal of the electric field, and (2) those "sensitive" to an electric field, that is, visible only with an applied field. Some of the latter were polarity dependent and some became more visible with an increase of electric field intensity.

P-N junctions in silicon have been inspected by Thiessen and Tuyen using nematic liquid crystals (Ref. 60). Electric field induced scattering was used for

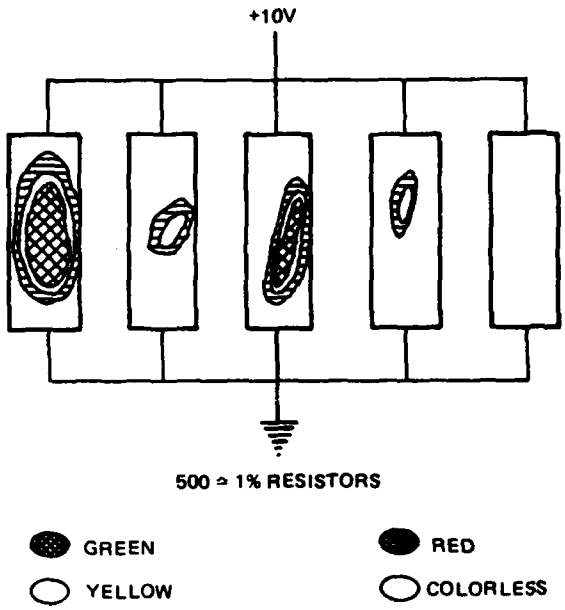

Figure 55. Temperature Distribution Pattern on Operating Resistors (From Ref. 30, Reproduced by Permission of The American Society for Nondestructive Testing, Inc., Columbus, OH)

contactless determination of their reverse voltage characteristics. Uniformity of diode structures and junctions and the quality of photodiodes were investigated. Pinholes having diameters of 1 μm were easily detected in SiO_2, although exact determination of size was difficult because turbulent areas tend to be larger than the defect. With higher voltages, thin spots which were not actually punctures were also detectable. Layers of Al_2O_3 and Si_3N_4 were also successfully investigated.

Chips containing diodes were tested for uniformity using the same test cell. The diodes were reverse biased, and so long as the resistances of the diodes were high, the voltage drop in the liquid crystal was below that required for turbulence. The high resistance of the liquid crystal prevents cross coupling. With increasing voltage the diodes appear gradually, those with the lowest reverse impedance first. Quantitative data was obtained by comparing the reverse characteristics, but uniformity could be determined at a single glance.

A photodiode was also tested. The radiation was detected on the photo-sensitive side via an opening in the metal substrate. The reverse voltage was adjusted so that scattering did not occur. However, the voltage across the sandwich was above that required for dynamic scattering. Upon illumination of the photodiode, the voltage produced across the liquid crystal layer caused scattering.

3. Integrated Circuits

A very versatile and easy means for testing defects in silicon dioxide layers on integrated circuits was reported by Keen (Ref. 44). He placed a thin film of the nematic phase MBBA between the wafer to be tested and a tin oxide coated slide, as shown in Figure 56. When a

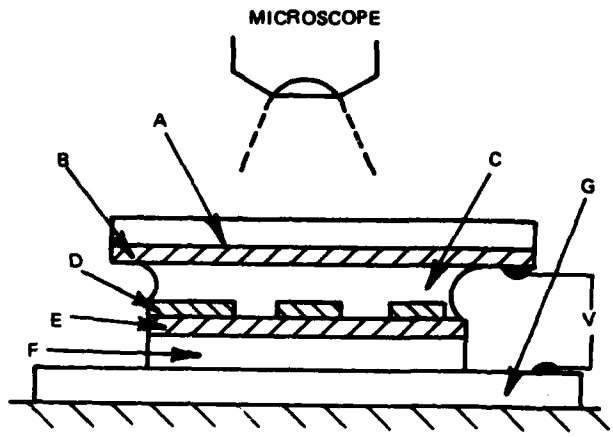

A MICROSCOPE COVER SLIDE
B TIN-OXIDE COATING
C NEMATIC LIQUID CRYSTAL (M.B.B.A.)
D METALLISATION PATTERN
E DIELECTRIC LAYER
F SILICON SUBSTRATE
G STAINLESS-STEEL SLIDE
V STABILIZED VOLTAGE SOURCE

Figure 56. Experimental Arrangement for Testing Defects in Silicon Dioxide Layers on Integrated Circuits (From Ref. 44, Reproduced by Permission of the Controller of Her Britannic Majesty's Stationery Office, London [British Crown Copyright])

voltage was applied, defects could be seen as highly turbulent liquid crystal regions. A voltage of 7 to 8 volts was required for pinholes (no insulation layer at all), with higher voltages needed for incomplete defects such as thin spots. Once the fault was located the applied voltage was removed, the induced turbulence ceased, and the fault could be examined by other means, as desired. Since the turbulence was only at a fault, different types of defects such as pinholes, scratches, metallization isolation, substrate connections, etc., could be identified.

Figure 57 shows a display on a multiple-gate m-n-o-s structure fabricated from 600 ohm meter (6 ohm-cm) n-type silicon and having a 600 nm aluminum metallization. A wafer, containing 61 chips of the multiple-gate m-n-o-s structure, shown in Figure 54 was tested first by the liquid crystal technique and then by conventional manual probing using a curve tracer. There was exact correlation between the results on 831 of 854 gates, of which 166 were found to be faulty. The twenty-three gates which had been observed to leak by the liquid-crystal technique but not when probe tested were re-

Figure 57. Detection of Faults on a Multiple Gate–M-N-O-S Structure Using MBBA (From Ref. 44, Photograph Used by Permission of the Controller of Her Britannic Majesty's Stationery Office, London [British Crown Copyright])

examined by the liquid-crystal technique to reveal that (1) two of the discrepancies were caused by breaks in the metallization, so that the pads (which were probed) were isolated even though the gates were leaking, (2) eighteen gates which showed faulty when first examined were insulating upon probe testing, and (3) three gates were still leaking. Four of the eighteen gates which had changed were closely inspected revealing pinholes 2-6 μm in diameter in the aluminum metallization and pitting in the underlying bitride layer on four, apparently caused by self-healing during the probe testing. The other 14 gates had self-healed with insufficient force to punch holes. Of the three remaining gates which were still leaking (by the liquid crystal tests), one had no leakage detectable by probing, another had 250 nA leakage, the detection limit, and the third had a diode characteristic, so that the initial probe may have used the wrong polarity.

This and other experiments indicated that (1) the liquid-crystal technique has greater sensitivity, (2) the technique is a very useful diagnostic method, and (3) correlation with conventional probe testing is excellent. A very quick assessment of a circuit or whole wafer can be made since the results are visual. This method can be used to obtain electrical as well as topographical data and can replace routine optical methods.

An effective method for locating oxide defects on integrated circuits has been reported by Ebel and Engelke (Ref. 61). A thin layer of nematic liquid crystal was placed on the device being analyzed and was covered by a sheet of glass with a thin transparent, conductive coating such as tin oxide with the conductive side in contact with the liquid crystal. A voltage source was connected between the substrate of the device and the conductive layer. An immediate disturbed area occurred wherever current flowed. Figure 58 shows the basic arrangement. When coated with a liquid crystal and a voltage was applied, vortices formed, including areas above contact windows, as expected, and over a pinhole. This can be seen in Figure 59. No oxide failure

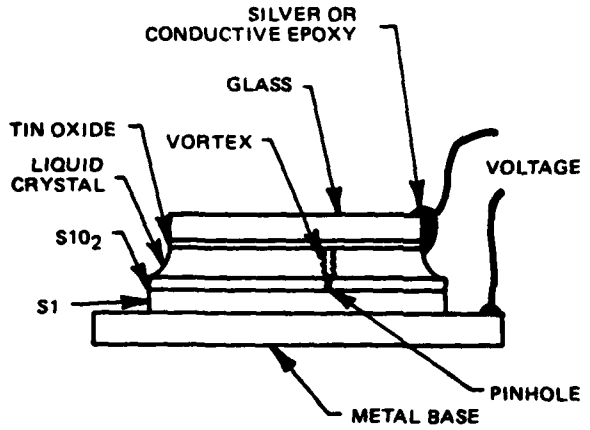

Figure 58. Schematic of Liquid Crystal Instrumentation for Locating Oxide Defects on Integrated Circuits (From Ref. 61, Reproduced with Corrections as Suggested by Original Author and by Permission of The Institute of Electrical and Electronics Engineers, Inc., N Y)

was found under a 1000x optical microscope, but a pinhole having a diameter of approximately 0.5 μm was found with a scanning electron microscope, thus demonstrating the resolution available with the liquid crystals.

The application of cholesteric liquid crystals to integrated circuit inspection has been investigated by Garbarino and Sandison (Ref. 62). A schematic of the set up for testing is shown in Figure 60. The liquid crystal was mixed with a volatile suspension medium and applied to the chip either with an eyedropper or an air brush to a thickness of 3-5 μm. The film was continuous and kept as uniform in thickness as possible. A crystal thickness of more than 10 μm allowed thermal diffusion to degrade the resolution. The temperature of the substage was held at 2°C below the transition temperature of the crystal by the assembly shown in Figure 61. The device was then powered so the temperature at the short was in the color range of the

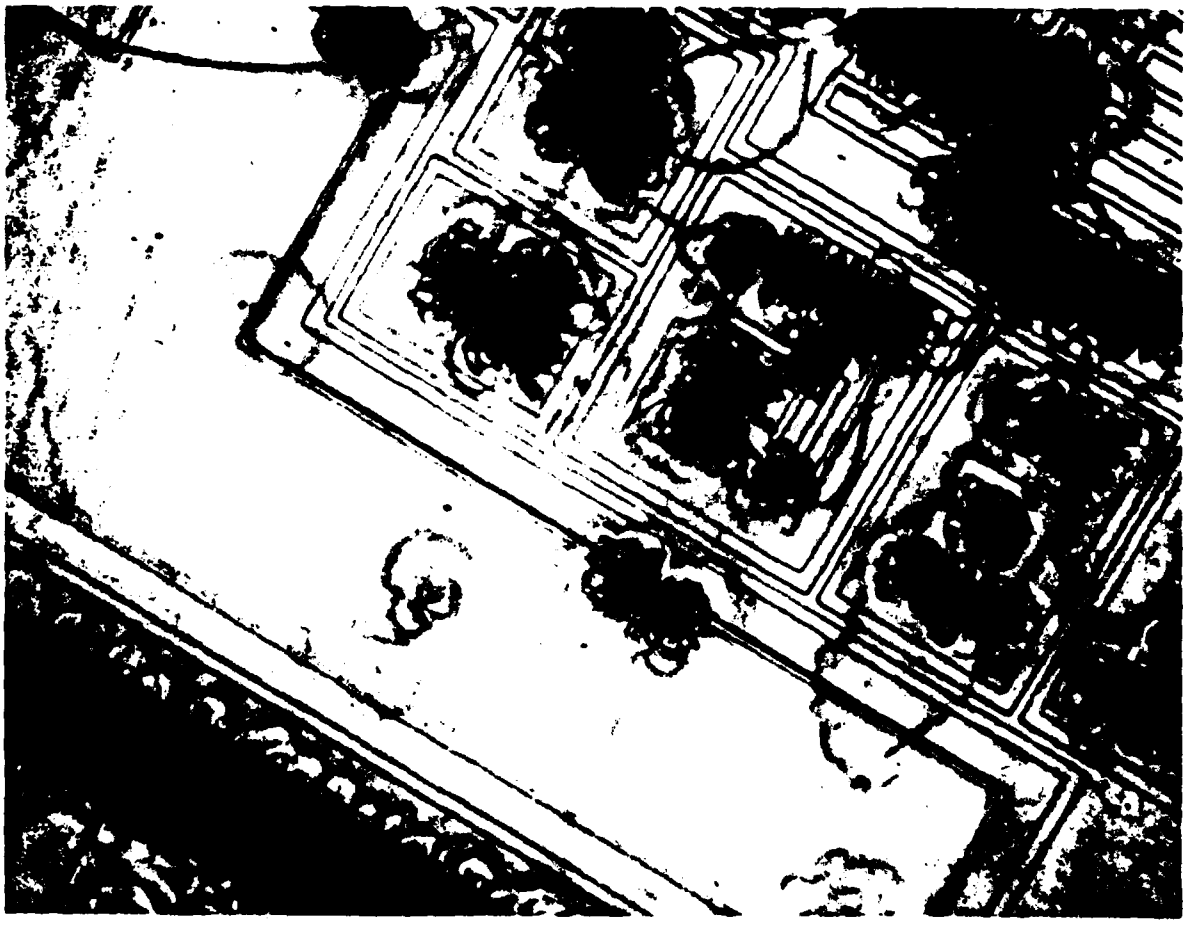

Figure 59. Liquid Crystal Test for Pinholes in Oxides Voltage Applied [Vortex Forms at Pinhole]
(From Ref. 61, Photograph Used by Permission of The Institute of Electrical and Electronics Engineers, Inc., N Y)

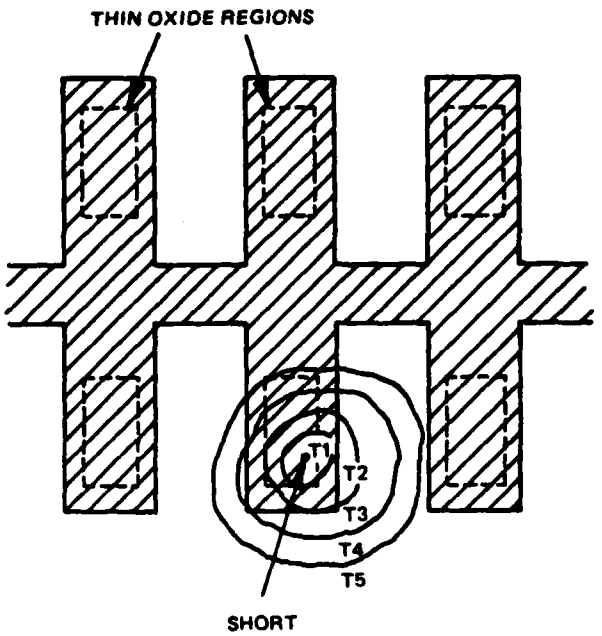

Figure 60. Side View (Cutaway) of Header-Substage Assembly Used to Provide Temperature Control (From Ref. 62, Reproduced by Permission of The Electrochemical Society, Inc., Publisher, Princeton, N J)

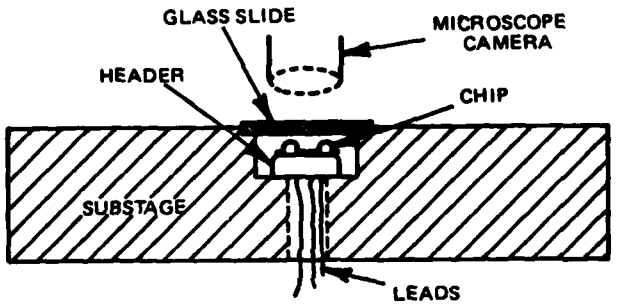

Figure 61. Schematic of a Defective Gate Chain. The Cross-Hatched Areas Indicate the Metalization Pattern Forming the Chain. Gate Areas are Outlined by Dashed Lines. The Rough Circles Around the Short Represent Isotherms of the Temperature Profile Around the Powered Short. Temperatures T1 > T2 > – > T5 are the Average Temperatures in Their Respective Regions. Under Action of the Liquid Crystal Region 1 will appear blue; Region 2, Green; Region 3, Yellow; Region 4, Red; and Region 5, Colorless (From Ref. 62, Reproduced by Permission of The Electrochemical Society, Inc., Publisher, Princeton, N J)

material. A 0.2 to 0.4 μm layer of carbon black on the chip was used to absorb unscattered light.

Channin has reported use of nematic liquid crystals to view both electric fields and temperature distributions in integrated circuits with conventional microscopes (Ref. 63). The method was reported to be flexible, economic, and useable while circuits are operated at normal voltage and current ratings. Circuits were viewed with a conventional microscope using a crossed polarizer-analyzer pair. An image was formed by light which passed through the liquid crystal and reflected from the integrated circuit surface. Undistorted regions of the circuit showed darker because the light was unaffected, but where circuit operation disturbed the index of refraction, the polarization was altered and light seen, the amount depending on the magnitude and nature of the disturbance. For these experiments, MBBA was used. MBBA has negative dielectric anisotropy, meaning the molecules rotate to align perpendicular to an electric field. At a voltage between 3 and 10 volts, a threshold occurs at which the optical effects begin. At a voltage several times the critical voltage, saturation will occur. Between threshold and saturation, the degree of brightness is a qualitative indication of the magnitude of the field. In order to maintain a nonzero average response, an a.c. voltage must be used. (Charge accumulation on the SiO_2 layer covering the circuit produces a self-cancelling field). If the temperature of the liquid crystal is near the nematic-isotropic phase transition temperature, the alignment is also disturbed.

Zakzouk, Stuart, and Eccleston have used liquid crystals to study localized regions of high conductivity in thermally grown silicon dioxide on n-type silicon (Ref. 64). The approach used was very similar to that of Keen (Ref. 44). They reported a very strong polarity dependence of the turbulence, and thus the number of defects seen, in 100 nm (0.1 μm) oxide films. In one sample, only one defect was seen with one set of polarities, but when the polarity was reversed, a much larger number of turbulencies was evident. The additional sites were generally not distinguishable under visual examination and they may have been caused by material defects (such as migration of positive ions of sodium through the oxide film) rather than voids or thin spots. The additional turbulent spots became more visible after extended stress. Quantitative analysis of these defects was possible using the liquid crystal.

Kapfer, Burns, Salvo, and Doyle have reported two years use of nematic liquid crystals for locating pinholes in thin and field oxide regions of MOS and bipolar integrated circuits (Ref. 65). In an MOS transistor, thin oxide coatings are about 0.1 μm thick and "field" oxide coatings are about 1 μm thick for both bipolar and MOS devices. Figure 62 is a sketch of a typical MOS device and shows the features of interest. The use of liquid crystals eliminates many of the procedures previously required to analyze failures. To perform these tests a liquid crystal cell as in Figure 63 was used. Glassivation and metallization layers were removed to expose oxide areas of interest. The liquid crystal material MBBA (one

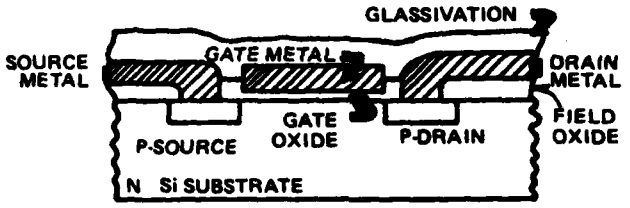

Figure 62. Typical P-MOS Transistor Cross-Section. The Glassivation is Deposited SiO_2. The Field and Gate Oxides are Thermally Grown SiO_2 (From Ref. 65, Reproduced by Permission of Rome Air Development Center, Griffiss AFB, N Y)

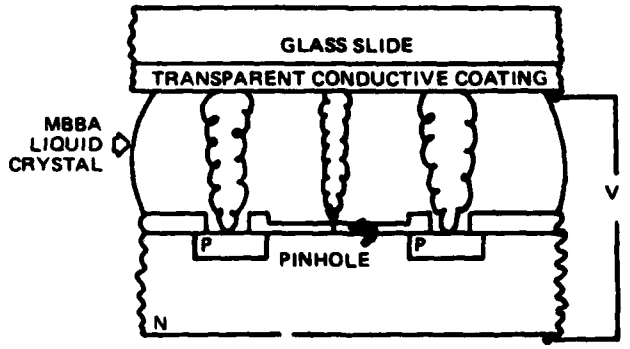

Figure 63. Basic Liquid Crystal Cell Used for Inspection of MOS and Bipolar Integrated Circuits. The Cell is Illuminated and Viewed from the Top Through a Microscope. The Large Oxide Openings are Contact Cuts Made to Allow the Conductor to Make Contact to Source and Drain Regions (From Ref. 65, Reproduced by Permission of Rome Air Development Center, Griffiss AFB, N Y)

drop) was placed on the device surface and a glass slide with a transparent conductive coating on one surface formed the top of the cell. Where openings in the insulating oxide occurred, a very small current flowed through the liquid crystal upon application of a voltage, resulting in localized turbulence, and hence dynamic scattering. Under a microscope, turbulences at the openings in the oxide layer appeared as dark vortices against a light background using dark field illumination. Vortices were larger than the openings in the oxide, making the holes appear larger than they actually were. This "magnification" allowed viewing of submicron defects normally not seen with optical microscopy.

C. Other NDE and Detection Applications of Liquid Crystals

1. RF and Microwave Imaging

Liquid crystals have been used to image and detect radiofrequency and microwave fields.

Advantages of liquid crystals for rf and microwave imaging are (1) direct observation of higher order modes, (2) direct observation of standing wave patterns on microwave strips and modules, and (3) imaging in side-looking radar. The first two may allow more precise NDE of waveguides and strips. Such a detector (1) can work in real time and (2) allows continuous sampling.

Sethares and Stiglitz reported the visual observation of high dielectric resonator modes using encapsulated cholesteric liquid crystals in the detector shown in Figure 64 (Ref. 66). Modes for frequencies on the order of 2 GHz were imaged and photographed. Sethares and Gulaya also have reported the observation of rf magnetic fields with cholesteric materials (Ref. 67).

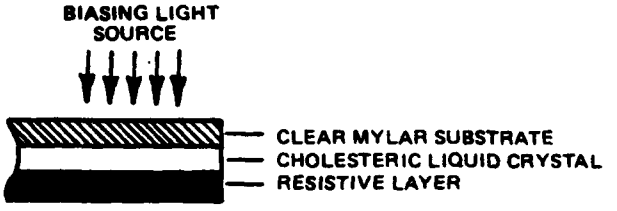

Figure 64. Cross Section of Liquid Crystal Detector Plate (From Ref. 66, Reproduced by Permission of Optical Society of America, Washington, D C)

A real time color display of microwave field patterns using cholesteric liquid crystals was reported by Augustine (Ref. 68) and by Augustine and Jaeckle (Ref. 69). It was used to plot near-field antenna patterns and mode patterns in complex waveguides and resonators, and to measure impedance and power by detecting standing waves and power-density patterns in open transmission lines. The device was made from a very thin Mylar membrane whose size depended on the experiment. For a small rectangular waveguide a 152 mm (6 in.) diameter membrane was used. A thin metallized film deposited on one side of the membrane was coated with the liquid crystals. A concentrated microwave beam passing through the membrane set up currents in the metallized film which were then very locally converted to heat in proportion to the amount of energy absorbed. Distinct color regions formed a two-dimensional plot of the microwave field intensity.

Among projected applications were:

(1) Antenna near-field and far-field analysis,
(2) Plotting of mode patterns in complex waveguides, resonators, and transmission media,
(3) Fault detection in dielectric materials and radomes,
(4) Microwave holography, and
(5) Microwave imaging.

Augustine and Kock have also reported microwave holograms for power levels of 1.5 W/m^2(1 $mw/in.^2$) using cholesterics (Ref. 70).

Torkan reported the use of liquid crystals to rapidly map microwave field patterns (Ref. 71). Cholesteric liquid crystals coated over a resistive mylar film were used in various mixtures. A uniform layer of Nichrome was used to provide an impedance match to microwaves, thus heating the liquid crystal and providing a color display. Temperature biasing was by a.c. or d.c. currents in the lossy film or by illumination by a floodlight. Such a bias increases sensitivity and reduces incident microwave power requirements.

Fanslow reported that cholesteric liquid crystals having color range centered at different temperatures have been coated on both metallized and non-metallized plastic disks respectively, and used to monitor microwave radiation at 2.45 GHz at power density levels of 1.5 to 23.3 W/m^2 (1 to 15 mW/cm^2) (Ref. 72). The metallized disk responds to both microwave radiation and ambient temperature while the non-metallized disk responds only to the latter; consequently, the difference in response is a measure of the microwave energy.

2. Viewing Infrared Energy

By viewing infrared energy, many nondestructive analyses can be made. Imaging of laser outputs, noncoherent inherently emitted radiation, holographic imagery, and interferometric patterns are all potentially useful.

The use of a cholesteric liquid crystal viewer to observe the far-field pattern of a HeNe laser at 3.39 μm was reported by Hansen, Fergason, and Okaya (Ref. 73).

Noncoherent energy can also be imaged. Ennulat and Fergason have reported the use of cholesteric liquid crystals (cholesteryl oleyl carbonate) to image with 0.2°C resolution against a 300K background using inherently emitted radiation (Ref. 74). Figure 65 shows the laboratory thermal imaging device. The infrared image of the scene is focused on a membrane and converted by absorption into a corresponding heat pattern. This pattern is reproduced in the liquid crystal deposited on the opposite side of the membrane. The membrane is enclosed in a temperature controlled chamber to keep the liquid crystal at the proper operating temperature. Illumination is accomplished with a visible monochromatic light source, thus highlighting that particular color (temperature) and providing lower

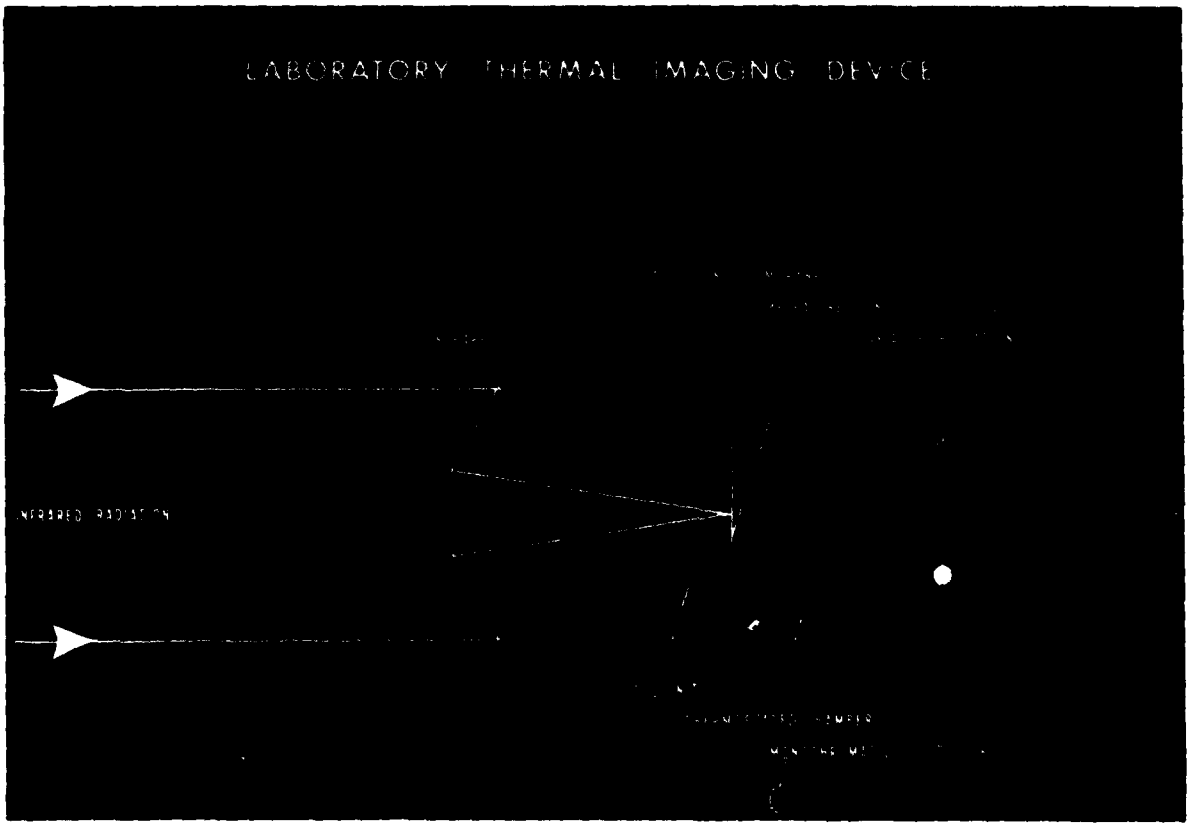

Figure 65. Laboratory Thermal Imaging Device (From Ref. 74, Photograph Used by Permission of Gordon and Breach, Science Publishers, Inc., N Y)

intensity scattering for other temperatures (colors). Fine tuning of the temperature of the liquid crystal, and thus the actual temperature which is imaged, is accomplished by a radiation heater. This radiographic imaging technique could be used in many NDE applications, for example, (1) viewing structural faults, or (2) evaluating hot spots in electronic circuitry. It has the advantage of being much less expensive than conventional infrared imaging devices. The authors estimated that temperature differences as small as 0.02 K (0.02 °C) can be detected with improved lighting.

Additional reports of the visual observation of infrared and submillimeter wave laser beams using cholesteric liquid crystals have been made. Keilmann and Renk describe a thermal image converter for infrared and submillimeter wave radiation (Ref. 75). The energy density for full contrast was 40J/m² (0.004 J/cm²). The detector consisted of a 3 μm thick plastic membrane, a thin (3nm) layer of chromium, and a liquid crystal layer of 5-10 μm. An absorption of approximately 45% was achieved from 632.8 nm (a HeNe laser) to an X-band klystron at 3 cm.

Two additional reports, one by McColl (Ref. 76) and the other by Horton (Ref. 77), discuss the use of liquid crystals for detection of infrared radiation. The former suggests, in addition to the thermal response, that tunable filters for optical processing might be feasible. The latter discusses a water cooled IR imaging device which was used to view CO_2 laser radiation with a very good resolution suitable for IR holography, diffraction studies, and testing of infrared optical system resolution.

Thin membrane displays using cholesteric liquid crystals for the display of infrared laser beams have been developed by Stocker (Ref. 78). There is a tradeoff between rise time, decay time, resolution and sensitivity, the principal limiting factors being membrane thickness and surface cooling.

More recently, Margerum, Little, and Braatz have reported extensive work on development of a pyroelectric film/liquid crystal detector for CO_2 laser radiation (Ref. 79). Both cholesteric and nematic materials were considered and several designs were investigated. Responsivities as high as 1.2 μA/W were achieved with a one-inch device and a matrix of 10,000 elements.

Kobayashi and Sakusabe have reported that both Fabry-Perot and Mach-Zender interferograms have been made using the liquid crystal detector (Ref. 80). Infrared windows which are opaque in the visible range have been inspected using Fabry-Perot interferometry. A shadowgram of the fault was displayed on the detector. Minimum detectable void size was about 30 μm.

In what was apparently the first report of infrared holography, Simpson and Deeds described how a hologram was formed using a low power (1 watt) 10.6 μm CO_2 laser and a cholesteric liquid crystal medium sandwiched between glass and sodium chloride plates (Ref. 81). The hologram was simultaneously reconstructed with a HeNe laser at 632.8 nm. The sandwich was necessary (1) to protect the cholesteric liquid crystal, which was subject to deterioration when exposed to air, (2) to prevent drying of the cholesteric, as , when dry, it looked like waxed paper and strongly diffused incident light, and (3) to ensure a uniformly thick coating. Figure 66 shows the equipment. The CO_2 laser beam was split by a beamsplitter (uncoated NaCl).

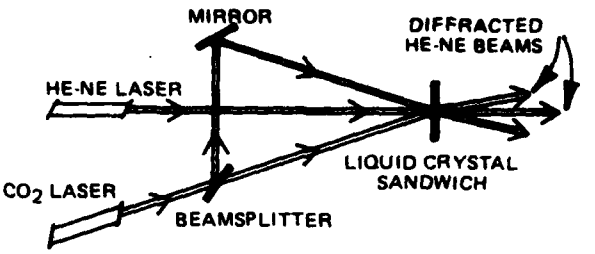

Figure 66. Arrangement of Equipment for Infrared Holography (From Ref. 81, Reproduced by Permission of Optical Society of America, Washington, D C)

The two resultant wavefronts were recombined in the liquid crystal sandwich with the beamsplitter providing an intensity ratio of transmitted to reflected beam of approximately 20:1. The He-Ne laser beam passed through the liquid crystals within the region of interference of the CO_2 laser beams. The He-Ne beam was unaffected when only one CO_2 beam was present, but with both IR beams the transmitted pattern consisted of the zero-order He-Ne beam plus two side beams. The latter corresponded to the first-order diffraction of the interference pattern between the two CO_2 laser beams.

Another report of CO_2 laser holograms being reconstructed using cholesteric liquid crystals and a HeNe laser has been made by Sakusabe and Kobayashi using the same apparatus as for the interferograms discussed in preceding paragraphs (Ref. 82). In this instance the hologram, as produced on the liquid crystal, was recorded photographically and then reconstructed, rather than displayed in real time. A liquid crystal area detector was made by stretching a 10 μm thick blackened vinyl sheet over a 120 mm diameter frame. A thin layer of liquid crystals was applied uniformly over the vinyl. Figure 67 shows the detector and Figure 68 (from Ref. 80) the IR transmission of the detector membrane including the liquid crystal. Most of the loss was by absorption. For viewing 10 μm radiation, a good visual indication with a spatial resolution of about 0.3 mm was obtained with about 100 W/m² (10 mw/cm²) incident power density. Response time was 0.5

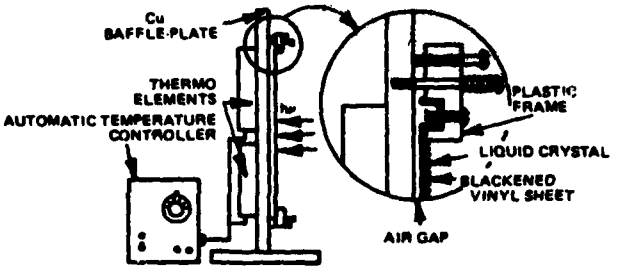

Figure 67. Construction of the Liquid Crystal Detector and Cross Sectional View of Variable Air Gap Between Cu-Plate and Membrane (From Ref. 80, Reproduced by Permission of Author–Paper Published at EOSD Conference 1971, East N Y, September 14-16, 1971)

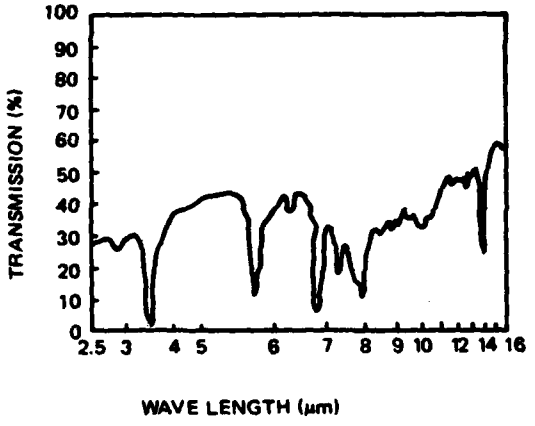

Figure 68. Curve of IR Transmission of the Membrane Including Both the Liquid Crystal and Vinyl Sheet (From Ref. 80, Reproduced by Permission of Author–Paper Published at EOSD Conference 1971, East N Y, September 14-16, 1971)

seconds. The optical system used for IR holography is shown in Figure 69. The hologram is displayed on the liquid crystal detector and photographed, was then reconstructed using a red helium-neon laser as shown.

3. Medical Applications

In addition to the example cited in Section III.A.1, several other investigations of the application of liquid crystals to medicine have been made, two examples of which are described here.

Liquid crystals have been used to map the temperature field produced by a cryosurgical probe. This was investigated by Petrovic by imbedding the probe in a clear gelatin-water test medium which simulated tissue (Ref. 83). A thin mylar sheet sprayed with a cholesteric liquid crystal was used for the mapping. Probe temperatures varied from -36°C to -117°C.

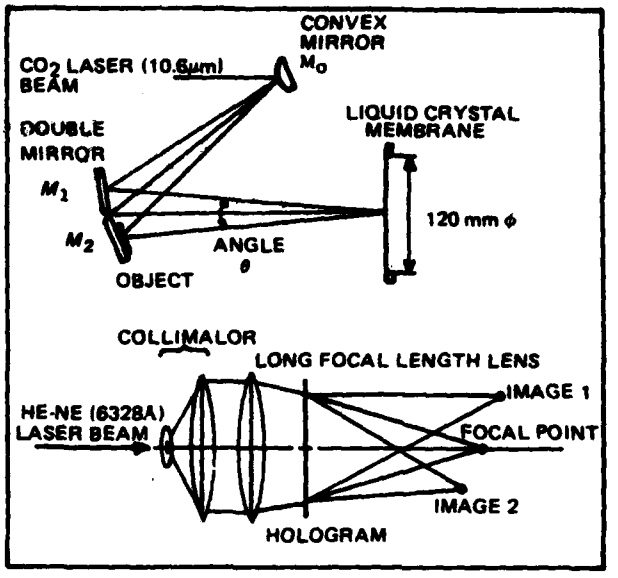

Figure 69. Optical Systems for Obtaining the IR Hologram (Above) and the Images (Bottom) (From Ref. 80, Reproduced by Permission of Author–Paper Published at EOSD Conference 1971, East N Y, September 14-16, 1971)

Correlation between the temperature as measured by calibrated liquid crystals and theoretical values was excellent.

Jeudy and Robillard have studied the variation of light scattered by nematic-cholesteric mixtures of liquid crystals and the application of this phenomenon to blood pressure measurement (Ref. 84). Temperature variation effects can be minimized or eliminated while enhancing pressure sensitivity by use of the proper mixtures. Research on this application is continuing.

V. THE FUTURE OF LIQUID CRYSTALS IN NDE

As can be seen from the work reviewed, there are many areas where the best method for inspection may be the use of liquid crystals. Add to this the number of supplementary uses and it can be seen that the potential impact of liquid crystals on NDE is great. A quick search of just one commercial literature retrieval database has indicated that, in 1977, the total number of articles published on liquid crystals approaches, if not exceeds, one thousand. This activity is certain to have an impact on the use of liquid crystals for NDE. This vast technical knowledge, coupled with ease of use and low cost, signals a steady growth of liquid crystal NDE as more people become familiar with its capabilities for both qualitative and quantitative evaluations and gain skill in its use.

VI. REFERENCES

1. F. Reinitzer, "Beitrage zur Kenntniss des Cholesterins," *Monatsh.*, Vol. 9, p. 421, 1888.
2. O. Lehmann, "Uber Fliessende Krystalle," *Z. Phys. Chem.*, Vol. 4, p. 462, 1889.
3. G. Friedel, "The Mesomorphic States of Matter," *Ann. Physique*, Vol. 18, p. 273, 1922.
4. G.H. Brown, "Structure, Properties, and Some Applications of Liquid Crystals," *J. Opt. Soc. Am.*, Vol. 63, No. 12, pp. 1505-14, Dec. 73.
5. G.H. Brown, "The Second International Liquid Crystal Conference," *J. Nondest. Test.*, Vol. 1, pp. 173-189, 1969.
6. V.I. Lebedev, V.I. Mordasov, and M.G. Tomilin, "Liquid Crystals in Optics," *Sov. J. Opt. Technol.*, Vol. 41, No. 7, pp. 403-12, Jul. 74.
7. W.E. Woodmansee, "Cholesteric Liquid Crystals and Their Application to Thermal Nondestructive Testing," *Mat. Eval.*, Vol. 24, pp. 564-6, 571-2, Oct. 66; this work was originally reported in AD705444.
8. Anon., "Liquid Crystals Take on a New Glow," *Chem. Week*, pp. 81-4, Nov. 76.
9. James L. Fergason, "Liquid Crystals," *Scient. Amer.*, Vol. 211, No. 2, pp. 76-85, Aug. 64.
10. G.H. Brown, "Liquid Crystals," *Ind. Res.*, pp. 53-8, May 66.
11. G.H. Brown and W.G. Shaw, "The Mesomorphic State: Liquid Crystals," *Chem. Rev.*, Vol. 57, No. 1, pp. 1049-1157, Feb. 57.
12. G.H. Brown, J.W. Doane, D.L. Fishel, V. Neff, and E. Drauglis, "Liquid Crystals," State-of-the-Art Report, Apr. 71, AD725949.
13. S. Chandrasekhar, "Liquid Crystals," *Rep. Prog. Phys.*, Vol. 39, No. 7, pp. 613-92, Jul. 76.
14. F.A. Jenkins and H.W. White, "Fundamentals of Optics," 3rd edition, McGraw-Hill Book Co., p. 495, 1957.
15. J.L. Fergason, "Cholesteric Structure-I, Optical Properties," *Molecular Crystals*, Vol. 1, No. 2, pp. 293-323, Apr. 66.
16. Y. Kagawa, T. Hatakeyama, and Y. Tanaka, "Detection and Visualization of Ultrasonic Fields and Vibrations by Means of Liquid Crystals," *J. Sound and Vibration*, Vol. 36, No. 3, pp. 407-16, 1974.
17. J.L. Fergason, "Liquid Crystals in Nondestructive Testing," *Appl. Opt.*, Vol. 7, No. 9, pp. 1729-37, Sep. 68.
18. J.L. Fergason, N.N. Goldberg, C.H. Jones, R.S. Rush, L.C. Scala, and F.Davis, "Detection of Liquid Crystal Gases (Reactive Materials)," Tech. Rpt. No. RADC-TR-64-569, Aug. 65, AD620940.
19. B.J. Bulkin, "Interaction of Small Molecules with Liquid Crystals: A Spectroscopic Study," Final Rpt., DA-AROD-31-124-73-G97, Aug. 76, AD029404.
20. C.H. Durney, C.C. Johnson, and J.L. Lords, "Liquid Crystal Fiberoptic Temperature Probe," Final Rpt. N00014-67-A-0325-0011, Jun. 75, ADA014655.
21. W. Schambeck, "Reliability Testing of Electronic Parts," AGARD Lectures Series No. 81 on Avionics Design for Reliability, Nov. 76.
22. W.E. Woodmansee, "Aerospace Thermal Mapping Applications of Liquid Crystals," *Appl. Opt.*, Vol. 7, No. 9, pp. 1721-27, Sep. 68.
23. A.H. Wirzburger, "An Environmental Heat Transfer Study of a Rocket Motor Storage Container System," Master's Thesis, Naval Postgraduate School, Monterey, CA., Dec. 72, AD758515.
24. R.J. Field, "Liquid Crystal Mapping of the Surface Temperature on a Heated Cylinder Placed in a Crossflow of Air," Master's Thesis, Naval Postgraduate School, Monterey, CA., Mar. 74, AD777862.
25. J.P. McComas, "Experimental Investigation of Found Effects on a Heated Cylinder in Crossflow," Master's Thesis, Naval Postgraduate School, Monterey, CA., Dec. 74, ADA004240.
26. T.E. Cooper, R.J. Field, and J.F. Meyer, "A Liquid Crystal Thermographic Study of a Heated Cylinder in Cross Flow," Annual Rpt., No. NPS-59Cg74111, Naval Postgraduate School, Monterey, CA., Nov. 74, ADA002458; this was subsequently reported in *J. Heat Transfer*, Aug. 75.
27. W.H. Batts, Jr., "Investigation of Gravitational Effects on a Variable Conductance Heat Pipe Utilizing Liquid Crystal Thermography," Master's Thesis, Naval Postgraduate School, Monterey, CA., Dec. 75, ADA021865.
28. M.D. Kelleher, "Effects of Gravity on Gas-Loaded Variable Conductance Heat Pipes," Final. rpt., FY75-76, NSF AG-496, Naval Postgraduate School, Monterey, CA., Mar. 77, ADA039185.
29. R.S. Owendoff, "Gravitational Effects on the Operation of a Variable Conductance Heat Pipe," Master's Thesis, Naval Postgraduate School, Monterey, CA., Mar. 77, ADA039354.
30. W.E. Woodmansee, "Cholesteric Liquid Crystals and Their Applications to Thermal Nondestruc-

tive Testing," *Mat. Eval.*, Vol. 24, pp. 564-72, Oct. 66.

31. W.E. Woodmansee and H.L. Southworth, "Detection of Material Discontinuities with Liquid Crystals," *Mat. Eval.*, Vol. 26, pp. 149-54, Aug. 68.
32. J.C. Manaranche, "A Comparative Study of Four Methods of Nondestructive Testing of Welds," *British J. of Nondest. Test.*, Vol. 15, No. 6, pp. 179-86, Nov. 73.
33. S.E. Cohen, "The Application of Liquid Crystals for Thermographic Testing of Bonded Structures," Prepared under Cont. No. NAS 8-2-8-20627 by Lockheed Georgia Co. for NASA, Sep. 67, N67 35747.
34. C.M. Forman, Practical Applications of Liquid Crystals," Rep. No. RS-TR-70-4, DA Proj. No. MIS99P50427382, May 70, AD878790.
35. M. Tanzer, A. Sturzenegger, A. Mlodozeniec, L. White, and E. Kopko, "Application of ROCHROME Liquid Crystal Tapes for Thermographic Testing of Bonded Structures," Final Rpt., Prepared by Hoffmann-LaRoche Inc. under Cont. NAS 8-26848, Jun. 72, N73-12451.
36. S.P. Brown, "Liquid Crystals for Nondestructive Testing of Composite Structures," taken from Non-Metallic Materials Selection, Application, and Environmental Effects, 1972, SAMPE, Azusa, CA., pp. 449-58.
37. N.A. Bekeshko, "Techniques and Equipment for Thermal Nondestructive Quality Control of Products and Materials," *Sov. J. Nondest. Test.*, Vol. 8, No. 4, pp. 465-70, Jul.-Aug. 72.
38. R.T. Schaum, "Development of a Nondestructive Inspection Technique for Advanced Composite Materials Using Cholesteric Liquid Crystals," Master's Thesis, Naval Postgraduate School, Monterey, CA., Sep. 76, ADA032322.
39. L.V. Best, "Use of Cholesteric Liquid Crystals for Locating Voids in Adhesively Bonded Helicopter Rotor Blades," Final rpt., Report No. USAMC-ITC-02-08-73-029, Mar. 74, AD785502.
40. A.P. Pontello, "Nondestructive Testing of Coalescers (Fuel Filters) on a Continuous Basis Using Liquid Crystals," ASME publication 72-DE-25, pp. 1-7.
41. A.P. Pontello, "Nondestructive Testing of Fuel Handling and Filtration Equipment Using Liquid Crystals and Thermography," Dept. of the Navy, Naval Air Propulsion Test Center, Trenton, N.J., 1973, AD772099.
42. A.L. Lavery, I. Litant, R.P. Ryan, N. Knable, H.L. Ceccon, "Survey of Nondestructive Tire Inspection Techniques," Cont. No. HS203, Report No. DOT- TSC-NHTSA-71-5, prepared for National Highway Traffic Safety Administration, Jul. 71, PB-213202.
43. J.P.G. Farr, J.M. Keen, and M.D. Pettitt, "A Nondestructive Optical Technique for Testing Lacquered Metal Surfaces," *Electrodeposition and Surface Treatment*, Vol. 1, pp. 449-55, Jul. 73.
44. J.M. Keen, "Nondestructive Optical Technique for Electrically Testing Insulated-Gate Integrated Circuits,"*Electronics Letters*, Vol. 7, No. 15, pp. 432-33, Jul. 71.
45. E.B. Singleton, "Measurement of Temperatures Developed in Tensile Bars Under Test to Fracture," Tech. Report No. 12121, Cont. No. DAAEO7-75-M-2132, Bowling Green State Univ., Dept. of Physics, Dec. 75, ADA040424.
46. E.J. Klein and A.P. Margozzi, "Exploratory Investigation on the Measurement of Skin Friction by Means of Liquid Crystals," Proc. XI Israel Ann. Conf. AVIATION and ASTRONAUTICS, Mar. 1969, Reprinted from *Israel Journal of Technology*, Vol. 7, No. 1-2, pp. 173-180, 1969.
47. E.C. Knox, "Measured Pressure Distributions on an 80-Deg. Swept Tetrahedron Body at Mach 5 and Angles of Attack to 10 Deg (U)," Fin. Rpt., AEDC-TR-69-246, Cont. No. F40600-69-C-0001, Aug. 69, AD505947.
48. R. Lemberg, "Liquid Crystals for the Visualization of Unsteady Boundary Layers," AFOSR Scientific Report,AFOSR-TR-71-2622, Themis Report N69-9, Themis Contract F44620-69-C-0022, May 71, AD737953.
49. E.J. Klein, "Application of Liquid Crystals to Boundary-Layer Flow Visualization," AIAA Paper No. 68-376, AIAA 3rd Aerodynamic Testing Conference, San Francisco, CA., Apr. 8-10, 1968.
50. W.H. Sproat and S.E. Cohen, "AGIS — An Acoustographic Imaging System," Mat. Eval., pp. 73-76, Apr. 70, presented at Spring Conference of American Society for Nondestructive Testing, Mar. 10-13, 1968, in Los Angeles, CA.
51. B.D. Cook and R.E. Werchan, "Mapping Ultrasonic Fields with Cholesteric Liquid Crystals" *Ultrasonics*, Vol. 9, No. 2, pp. 101-102, Apr. 71.
52. R.D. Maple, "Utilization of Temperature Sensitive Liquid Crystals for Thermal Analysis and an Application to Transducer Investigations," Research report, Naval Underwater Systems Center, Newport, R.I., May 72, AD744211.
53. Y. Kagawa, T. Hatakeyama, and Y. Tanaka, "Detection and Visualization of Ultrasonic Fields and Vibrations by Means of Liquid Crystals," *J.*

of Sound and Vibration, Vol. 36, No. 3, pp. 407-15, Oct. 1974.

54. J.C. Manaranche and P. Henry, "Visualisation of an Ultrasonic Beam by Means of Liquid Crystals," *British J. of NDT*, Vol. 18, No. 4, pp. 107-09, Jul. 76.
55. M.E. Fourney, D.C. Auth, M.J. Intlekofer, and A.S. Kobayashi, "Nondestructive Determination of Surface Flaw Geometry by Acoustical Holography, Exploratory Development," Tech. Rpt., prepared for Air Force Materials Laboratory, AFML-TR-73-129, Jun. 73, AD770108.
56. H. Mailer, K.L. Likins, M.J. Golis, and R.C. McMaster, "New Techniques of Acoustic Image Detection," *International Journal of Nondestructive Testing*, Vol. 4, No. 4, pp. 283-99, 1973.
57. F. Scudieri, S. Verginelli, and A. Ferrari, "Optical Visualization of Deformations with Nematic Liquid Crystals," *Appl. Phys.*, Vol. 11, No. 1, pp. 103-06, Sep. 76.
58. P.J. Marto and M.D. Kelleher, "The Thermal Performance of Air-Cooled Circuit Boards Used in Standard Electronic Package Designs," Final rpt., NPS-59Mx74051, Naval Postgraduate School, Monterey, CA., May 74, AD781365.
59. M. Lescinsky and J. Fridrich, "Investigation of Thin Film Capacitor Defects Using Nematic Liquid Crystals," *Thin Solid Films*, Vol. 14, No. 2, pp. S17-S19, 1972.
60. K. Thiessen and L. Tuyen, "Application of Nematic Liquid Crystals for the Investigation of p-n Junctions and Insulating Layers," *Phys. Stat. Sol. (a)*, Vol. 13, No. 73, 1972.
61. G.H. Ebel and H.A. Engelke, "Failure Analysis of Oxide Defects," 11th Annual Proc. of Reliability Physics 1973, Las Vegas, NV., Apr. 3-5, 1973, sponsored by IEEE Electron Devices Grp. and IEEE Reliability Grp., pp. 108-16.
62. P.L. Garbarino and R.D. Sandison, "Nondestructive Location of Oxide Breakdowns on MOSFET Structures," *J. Electrochem. Soc.*, Vol. 120, No. 6, pp. 834-5, Jun. 73.
63. D.J. Channin, "Liquid Crystal Technique for Observing Integrated-Circuit Operation," *IEEE Trans. on Electron Devices*, Vol. ED-21, No. 10, Oct. 74.
64. A.K. Zakzouk, R.A. Stuart, and W. Eccleston, "The Nature of Defects in Silicon Dioxide," *J. Electrochem. Soc.*, Vol. 123, No. 10, pp. 1551-56, Oct. 76; also A.K. Zakzouk, W. Eccleston and R.A. Stuart, "Polarity Dependent Oxide Defects Located Using Crystals," *Solid-State Electronics*, Vol. 19, No. 2, pp. 133-34, 1976.
65. V.C. Kapfer, D.J. Burns, C.J. Salvo, and E.A. Doyle, Jr., "Reliability Tests and Analysis of CMOS NOR Gates with Application of Nematic Liquid Crystal Failure Analysis Techniques," Tech. Rpt., RADC-TR-76-96, Griffiss AFB, New York, Jun. 76, ADA028519.
66. J.C. Sethares and M.R. Stiglitz, "Visual Observation of High Dielectric Resonator Modes," *Appl. Opt.*, Vol. 8, No. 12, Dec. 69.
67. J.C. Sethares and S. Gulaya, "Visual Observation of RF Magnetic Fields Using Cholesteric Liquid Crystals," ARCRL-71-0261, Apr. 71, reprinted from *Appl. Opt.*, Vol. 9, No. 12, pp. 2795-97, Dec. 70, AD723692.
68. C.F. Augustine, "Field Detector Works in Real Time," *Electronics*, Vol. 41, No. 13, Jun. 68.
69. C.F. Augustine and W.G. Jaeckle, "Real-Time Area Detection of Electromagnetic Fields Using Cholesteric Liquid Crystals," Abstracts of 18th Annual Symposium USAF Antenna Research and Development Program, Air Force Avionics Lab, Wright-Patterson AFB, OH., Oct. 68, AD846427.
70. C.F. Augustine and W.E. Kock, "Microwave Holograms Using Liquid Crystal Displays," *Proc. of the IEEE*, Vol. 57, No.3, Mar. 69, pp. 354-55.
71. H. Torkan, "Visual Detection of Microwave Field Patterns Using Liquid Crystals," Master's Thesis, Naval Postgraduate School, Monterey, CA., Sep. 70, AD717583.
72. G.E. Fanslow, "A Liquid Crystal Calorimeter for Radiation Monitoring," *J. of Microwave Power*, Vol. 11, No. 2, 1976, pp. 149-51.
73. J.R. Hansen, J.L. Fergason, and A. Okaya, "Display of Infrared Laser Patterns by a Liquid Crystal Viewer," *Appl. Opt.*, Vol. 3, No. 8,pp. 987-88, Aug. 64.
74. R.D. Ennulat and J.L. Fergason, "Thermal Radiography Utilizing Liquid Crystals," *Molecular Crystals and Liquid Crystals*, Vol. 13, No. 2, pp. 149-64, May 71.
75. F. Keilmann and K.F. Renk, "Visual Observation of Submillimeter Wave Laser Beams," *Appl. Phys. Letters*, Vol. 18, No. 10, pp. 452-54, May 71.
76. J.R. McColl, "A Review of the Unusual Optical Properties of Liquid Crystals," Proc. of the Special Meeting on Unconventional Infrared Detectors, Willow Run Laboratories of the Institute of Science and Technology, Univ. of Michigan, Ann Arbor, Apr. 71, AD726224.
77. R.F. Horton, "A Water-Cooled Cholesteric Liquid Crystal Infrared Imaging Devices," Proc. of the Special Meeting on Unconventional Infrared Detectors, Willow Run Laboratories of

the Institute of Science and Technology, Univ. of Michigan, Ann Arbor, Apr. 71, AD726224.

78. H.J. Stocker, "Liquid Crystal Displays for the Evaluation of CO_2 Lasers," Scientific Rpt., ARL-72-0081, Prepared for Aerospace Research Laboratories, May 72, AD752201.
79. J.D. Margerum, M.J. Little, and P.O. Braatz, "Pyroelectric Film Liquid Crystal Detector for 10.6 μm Region," Fin. Tech. Rpt., AFML-TR-74-268, Cont. No. F33615-73-C-5129, prepared for Air Force Materials Laboratory, No. 74, ADA007852.
80. S. Kobayashi and T. Sakusabe, "Infrared Interferometry Using Liquid Crystals and Their Applications to Nondestructive Testing on Semiconductors and Material Research," Proc. of the Technical Program, Electro-optical Systems Design Conference, 1971 East, New York, N.Y., Sep. 14-16, 1971, pp. 280-85.
81. W.A. Simpson and W.E. Deeds, "Real-Time Visual Reconstruction of Infrared Holograms," *Appl. Opt.*, Vol. 9, No. 2, pp. 499-501, Feb. 70.
82. T. Sakusabe and S. Kobayashi, "Infrared Holography with Liquid Crystals," reprinted from *Japanese Journal of Applied Physics*, Vol. 10, No. 6, pp. 758-61, Jun. 71.
83. W.K. Petrovic, "An Experimental Investigation of the Temperature Field Produced by a Surgical Cryoprobe," Master's Thesis, Naval Postgraduate School, Monterey, CA., Dec. 72, AD757251.
84. M.J. Jeudy and J.J. Robillard, "Light Scattering by Liquid Crystals Under Pressure Variations: Application to Blood Pressure Measurements," reprinted in *Opt. and Laser Technol.*, Vol. 8, No. 3, pp. 117-19, Jun. 76.